Journal of Dynamics, Monitoring and Diagnostics, 2026, 5, 156-183
https://doi.org/10.37965/jdmd.2026.1233

ISTP
RESEARCH ARTICLE

Railway Wheel Life Cycle Management: Design, Degradation, Monitoring, and Condition-Based Maintenance

Haotian Lyu,[1] Ruichen Wang,[1] Yating Han,[1] Shuai Zhang,[1] and David Crosbee[2]
[1]School of Mechanical Engineering, Shijiazhuang Tiedao University, Shijiazhuang 050043, China
[2]Institute of Railway Research, University of Huddersfield, Huddersfield, HD1 3DH, UK

(Received 28 February 2026; Revised 07 April 2026; Accepted 16 April 2026; Published online 18 April 2026)

Abstract: Increasing operating speed, axle load, and utilization intensify contact forces, creepages, and excitation frequencies at the wheel–rail interface, making tread and flange degradation a persistent challenge in modern railway operation. Railway wheels are safety-critical load-bearing components, and service performance is governed by coupled evolution of wear, rolling contact fatigue (RCF), out-of-roundness, and thermally influenced surface response under vehicle-track coupled dynamics. The review adopts a life cycle structure covering design and manufacture, in-service degradation with prediction, and condition monitoring with maintenance intervention. For design and manufacture, the discussion covers wheel steel design and heat treatment, profile design and equivalent conicity control, process routes with residual stress management, and durability under regional environments. For in-service operation, wheel–rail system matching, wear and profile evolution modeling, and RCF assessment are compared in terms of governing assumptions, required inputs, and applicability across operating regimes. For condition-based maintenance, the review links depot inspection, wayside, and on-board monitoring and decision rules to intervention options including turning, reprofiling, laser cladding repair, and surface strengthening. The review highlights a closed-loop view of wheel life management in which prediction, monitoring, and intervention are aligned against route-specific loading spectra, safety margin, and whole-life cost.

Keywords: condition monitoring; maintenance intervention; turning and reprofiling; wheel life cycle; wear prediction; wheel service performance

I. INTRODUCTION AND SCOPE

The rapid expansion of railway networks, together with sustained increases in operating speed, axle load, and traffic density, has made the wheel–rail interface one of the most critical locations governing the safety, efficiency, and durability of modern railway systems. Under increasingly demanding service conditions, tread wear, flange wear, out-of-roundness, and rolling contact fatigue (RCF) remain persistent challenges in both high-density passenger transport and heavy-haul freight operations. Such degradation arises from the combined action of wheel–rail contact mechanics, vehicle-track coupled dynamics, traction and braking loads, and environmental exposure and can affect running stability, ride quality, braking performance, maintenance demand, and the service life of both vehicle and track components.

Although substantial research has been devoted to railway wheel performance, most published studies remain focused on individual topics in isolation, including wear mechanisms, RCF assessment, profile optimization, condition monitoring, or repair technologies. Such a fragmented view is increasingly inadequate for modern railway applications, because wheel performance is inherently shaped by interactions across the full-service process. Material composition, manufacturing route, and initial geometry determine the starting condition of the wheel; operating conditions govern the evolution of contact state, damage accumulation, and near-surface response; maintenance actions repeatedly modify profile geometry and material condition over successive service cycles. A comprehensive understanding of wheel performance therefore requires a life cycle perspective capable of linking design, manufacture, operation, degradation, monitoring, and intervention within a unified technical framework [1–4].

From this standpoint, a life cycle-based review is valuable not only for organizing existing knowledge but also for clarifying the technical relationships among degradation mechanisms, condition indicators, predictive models, and maintenance strategies. The stage-based framework shown in Fig. 1 is therefore adopted to structure the present review. Section II examines the key design and manufacturing factors that define the initial wheel state. Section III reviews in-service degradation mechanisms and life prediction methods associated with wear and RCF. Section IV discusses condition monitoring and maintenance interventions that support condition-based maintenance (CBM). Section V summarizes the principal findings and highlights priority directions for future research. The purpose of this review is not just to compile previous studies but to provide a clearer technical logic for route-specific and system-specific wheel life management in modern railway systems.

II. DESIGN AND MANUFACTURE OF RAILWAY WHEELS

Railway wheels transmit vertical and lateral loads, provide guidance, and transfer traction and braking torque. Design and manufacturing choices therefore influence safety

Corresponding author: Ruichen Wangruichen (e-mail: ruichen.wang@stdu.edu.cn).

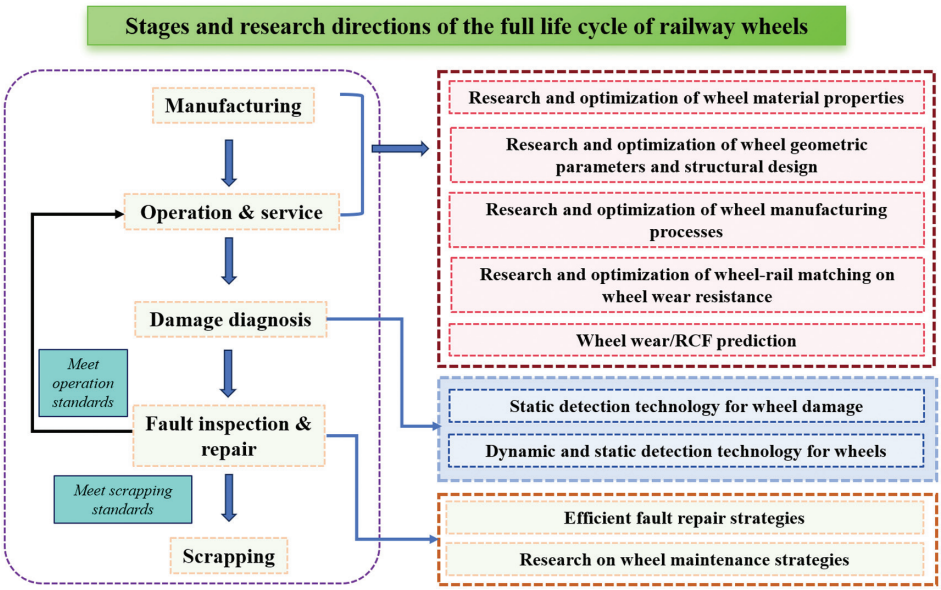

Fig 1. Full life cycle of train wheels and optimization directions.

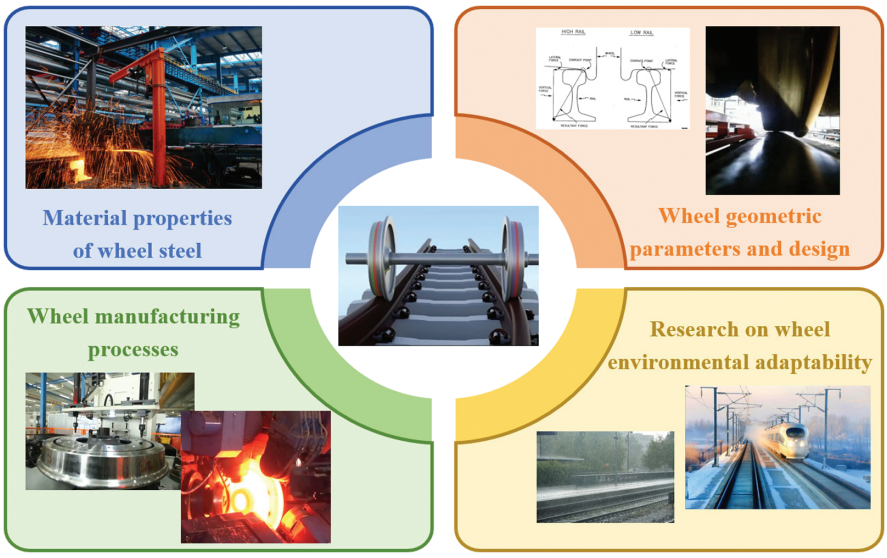

Fig 2. Research directions for wheel production and design.

margin, degradation rate, and maintenance demand over service life. Section II reviews four controllable levers before wheels enter service: material and microstructure, contact geometry through tread and flange design, manufacturing route with heat treatment and residual stress control, and durability under regional environments (Fig. 2).

A. WHEEL MATERIALS, MICROSTRUCTURE, AND ALLOY DESIGN

The material design of railway wheels has long been recognized as a key factor governing service performance and damage evolution. Material capability affects not only wear resistance, fatigue strength, fracture toughness, and resistance to thermally induced surface damage but also the near-surface response under repeated rolling contact, which plays a decisive role in wheel life. At the same time, wheel material behavior is strongly influenced by wheel–rail pairing, because hardness ratio and work-hardening capacity shape wear partition and damage mode at the contact interface. For this reason, research on wheel materials has extended from conventional pearlitic steels toward bainitic, carbide-free bainitic, and dual hardness concepts, with the aim of improving crack resistance and near-surface deformation characteristics without unacceptable loss of toughness. More recently, surface engineered systems and graded architectures have also attracted attention as possible routes for localized performance development in the contact layer. This section therefore reviews the main material systems and design strategies that have been explored for improving the service capability of railway wheels.

1). EFFECTS OF CHEMICAL COMPOSITION ON WEAR AND FATIGUE RESISTANCE. Pearlitic steel, characterized by a microstructure composed of pearlite, has long been widely used in railway wheels and rails. Owing to its lamellar ferrite/cementite structure, pearlitic steel shows excellent work-hardening capability and resistance to plastic deformation under rolling–sliding contact conditions. Studies have shown that by tailoring the carbon content and microalloying elements, such as silicon (Si), manganese (Mn), and chromium (Cr); it is possible to effectively refine the interlamellar spacing and optimize hardness distribution, thereby improving the wear resistance and RCF resistance of wheel steels. Extensive research has been conducted in this regard. Liu *et al.* [5] investigated the matching characteristics of four different wheel materials against rail steel and found that, as the carbon content of the wheel increased, the wheel hardness increased and the wear loss decreased, whereas the wear of the mating rail gradually increased. Chen *et al.* [6] carried out rolling contact simulation tests on four-wheel steels with carbon contents ranging from 0.51% to 0.72%. Their results showed that, with increasing carbon content, the hardness of the wheel increased, and the wheel wear depth gradually decreased as wheel hardness increased. Wang *et al.* [7] also reported that increasing carbon content can improve wheel hardness and wear resistance, but at the expense of aggravated rail wear. However, as the carbon content in wheel steel increases, the hardness and strength of the steel increase while its toughness decreases, resulting in reduced fatigue resistance of the wheel [8]. Although increasing carbon content can improve wheel hardness and reduce wheel wear, high carbon levels limit further hardness improvement and deteriorate toughness, making it difficult to achieve a balanced combination of strength and toughness and thereby weakening the wheel's resistance to fatigue damage.

In addition to adjusting the carbon content, the addition of microalloying elements such as Si, Mn, and Cr can also improve wheel strength. Sun *et al.* [9] compared the wear behavior of wheels made from conventional CL60 steel and newly developed CL60 steel with optimized Si, Mn, and Cr contents and additional Mo and V. The new CL60 steel wheels have been found and shown lower wear loss, total wear rate, and plastic deformation layer thickness than the original CL60 steel wheels. Pan *et al.* [10] proposed that increasing the Si content can improve the strength of wheel steel without impairing its plasticity and toughness. Zeng *et al.* [11] designed and prepared an improved wheel steel with high Si, high Mn, and low Cr contents, which revealed higher strength without compromising toughness. Demisie *et al.* [12] increased the contents of Si, Mn, and C in wheel steel and found that the steel achieved higher strength and hardness while retaining its original toughness. Carbon plays a decisive role in determining the properties of wheel steel. An increase in carbon content is beneficial for improving wear resistance, and a good balance between strength and toughness can be achieved when the carbon content is maintained within the range of 0.69%–0.74%. In addition to carbon, microalloying elements such as Si and Mn also apply significant effects on wheel steel performance; however, excessive additions can reduce wheel toughness [13].

Overall, the optimization of wheel steel has progressed from single carbon content regulation to a medium-carbon and microalloying-based design strategy, as shown in Fig. 3. Through precise control of trace element composition and microstructural tailoring, wear resistance can be improved while maintaining adequate toughness and fatigue performance. Meanwhile, increasing wheel strength g improves resistance to crack initiation but tends to reduce resistance to crack propagation. Such optimization strategies therefore continue to face an inherent trade-off between strength improvement and crack growth resistance. In particular, under conditions of high carbon or high alloy content, the accompanying reduction in material toughness limits the applicability of such steels in complex service environments associated with high speed and heavy-haul operations.

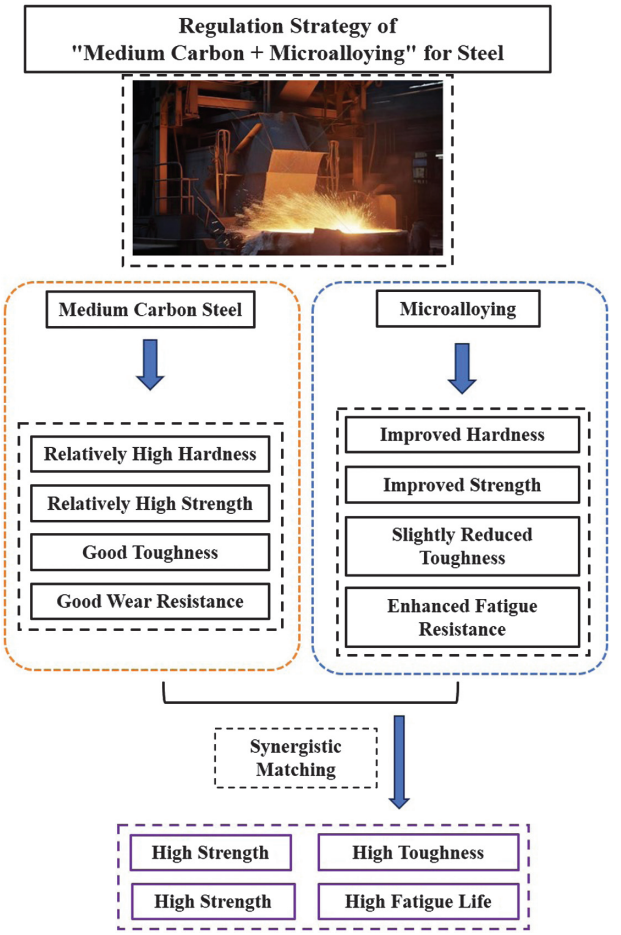

Fig 3. Regulation strategy of "Medium Carbon + Microalloying" for steel.

2). PEARLITIC AND BAINITIC WHEEL AND RAIL STEELS, WEAR MECHANISMS, AND MATERIAL PAIRING. At present, the improvement of pearlitic steel properties has gradually approached its theoretical limit. Although increasing carbon content can increase wear resistance, it often comes at the expense of toughness and may aggravate rail wear or even alter fatigue damage mechanisms. Therefore, while compositional optimization of conventional pearlitic steels still holds some potential, it is difficult to achieve breakthrough improvements in performance. Given that research on developing the mechanical properties of pearlitic steels has reached its theoretical ceiling, bainitic steels offering a combination of high strength, high toughness, and excellent wear resistance have emerged as promising alternatives [14,15]. Therefore, increasing attention has been directed toward bainitic steels, and extensive

Table I. Comparison of properties between pearlitic steel and bainitic steel

Steel type	Strength and hardness	Fatigue resistance	Crack growth rate	Ductility/ toughness	Wear resistance	Industrial application status
Pearlitic steel	Relatively high	Relatively high	Relatively fast	Relatively high	Excellent	Very mature
Bainitic steel	High	High	Relatively slow	High	Moderate	Under promotion

studies have been conducted worldwide to compare the wear behavior of steels with these two distinct microstructures. Singh *et al.* [16] investigated the mechanical properties of bainitic and pearlitic steels and found that bainitic rail steel exhibits superior strength, hardness, and impact toughness compared with pearlitic steel; however, its wear resistance was inferior. Lee *et al.* [17] compared the sliding wear behavior of bainitic and pearlitic steels and reported that, although bainitic steel has a higher initial hardness, pearlitic steel undergoes significant work hardening during wear, resulting in better wear resistance. Similarly, Viáfara *et al.* [18] confirmed through sliding wear tests that pearlitic steel exhibits superior wear resistance, which may be attributed to its stronger work-hardening capability. Zapata *et al.* [19] adjusted bainitic and pearlitic steels of different compositions to the same hardness level and conducted rolling wear tests. Under low load conditions, no significant difference in wear was observed; however, due to its superior work-hardening capability, bainitic steel exhibited better wear resistance in the later stages of testing. In recent years, considerable attention has been paid to carbide-free bainitic steels with high Si content for wheel–rail applications. Hasan *et al.* [20] studied the rolling/sliding wear behavior of two newly designed low-carbon, continuously cooled carbide-free bainitic steels and compared them with pearlitic steel. The results showed that bainitic steels indicates superior wear resistance, which increases with initial hardness. Sharma *et al.* [21] compared the wear performance of medium-carbon bainitic steel and pearlitic steel, demonstrating that bainitic steel possesses superior mechanical properties and improved wear resistance due to its higher hardness and strength. Chen *et al.* [22] investigated the evolution of near-surface microstructures and properties during sliding wear under different cooling conditions and found that bainitic steel exhibits better wear resistance than pearlitic steel under identical conditions. However, Liu *et al.* [23] reported that, despite the higher initial hardness of carbide-free bainitic rail steel, its wear loss exceeded that of pearlitic steel. The inferior wear resistance of bainitic steel was attributed to its relatively weaker work-hardening capability and the absence of a white etching layer (WEL) on its worn surface, whereas such a layer forms on pearlitic steel and contributes to improved wear resistance. Rezende *et al.* [24] studied wheel steels with different microstructures and found that bainitic steels exhibit lower mass loss, higher hardness, and greater capacity for accommodating plastic deformation. Moreover, the delamination wear process in bainitic steels develops more slowly, and crack propagation tends to remain closer to the surface. These findings indicate that highly localized plastic deformation in the surface layer of bainitic steel effectively suppresses crack initiation and propagation into the material depth. Zhang and Gu [25] developed a carbide-free bainitic steel wheel and demonstrated through rolling wear tests that the bainitic wheel–pearlitic rail combination exhibits superior wear performance compared with the pearlitic wheel–pearlitic rail pairing.

Overall, current studies indicate that wear behavior is governed not only by initial hardness but also by work-hardening capacity, plastic deformation, and the evolution of near-surface microstructures. The main property differences between pearlitic and bainitic steels are summarized in Table I. A simple one-to-one correlation between hardness and wear resistance cannot be assumed for steels with different microstructures, while wear performance is also influenced by the counterpart material. At present, no consistent conclusion can be drawn regarding the relative wear resistance of pearlitic and bainitic steels. In addition, comparative studies under representative service conditions remain insufficient. Future work can therefore focus on the systematic assessment of the overall service performance of wheel steels with different microstructures through full-scale field testing and wheel–rail system experiments.

3). EMERGING MATERIAL CONCEPTS AND SURFACE ENGINEERED SYSTEMS. To meet the future demands of railway transportation for lightweight structures, long service life, and ultra-high reliability, exploring novel solutions beyond traditional steel material systems has become an emerging trend. Composite materials, particularly metal matrix composites (MMCs), realized through architectural design and surface modification technologies, having significant potential for simultaneously improving strength, toughness, and wear resistance through microstructural innovation. Although these materials have not yet been widely applied to railway wheels, they provide valuable insights for the design of advanced surface engineering solutions. At present, notable progress has been achieved in the architectural design of MMCs (as shown in Fig. 4).

In terms of surface modification and coating reinforcement technologies, Movassagh-Alanagh *et al.* [26] used multilayer nanocomposite coatings on stainless steel using cathodic arc evaporation, combined with plasma nitriding of the substrate, thereby improving coating–substrate bonding strength and improving wear resistance. Ding *et al.* [27] developed a novel multiscale WC-10Co4Cr coating via high-velocity oxygen fuel (HVOF) spraying, consisting of nano-, submicron-, and micron-sized WC particles embedded in a CoCr matrix. The coating exhibited low porosity ($\leq$0.32%) and high fracture toughness. Ding *et al.* [28] fabricated h-BN/CaF_2/Fe composite coatings using laser cladding and evaluated their wear and RCF resistance through hardness and residual stress measurements. The results indicated that optimized compositional ratios increasing both wear and fatigue resistance. Wang *et al.* [29] produced a ~10 μm-thick nanocrystalline surface layer on low-carbon steel via surface mechanical grinding, resulting in a gradual hardness increase from the substrate to the surface. Under low loads, the friction coefficient was reduced, improving wear resistance. Wang [30] further demonstrated that laser quenching forms a hardened martensitic layer of controlled depth,

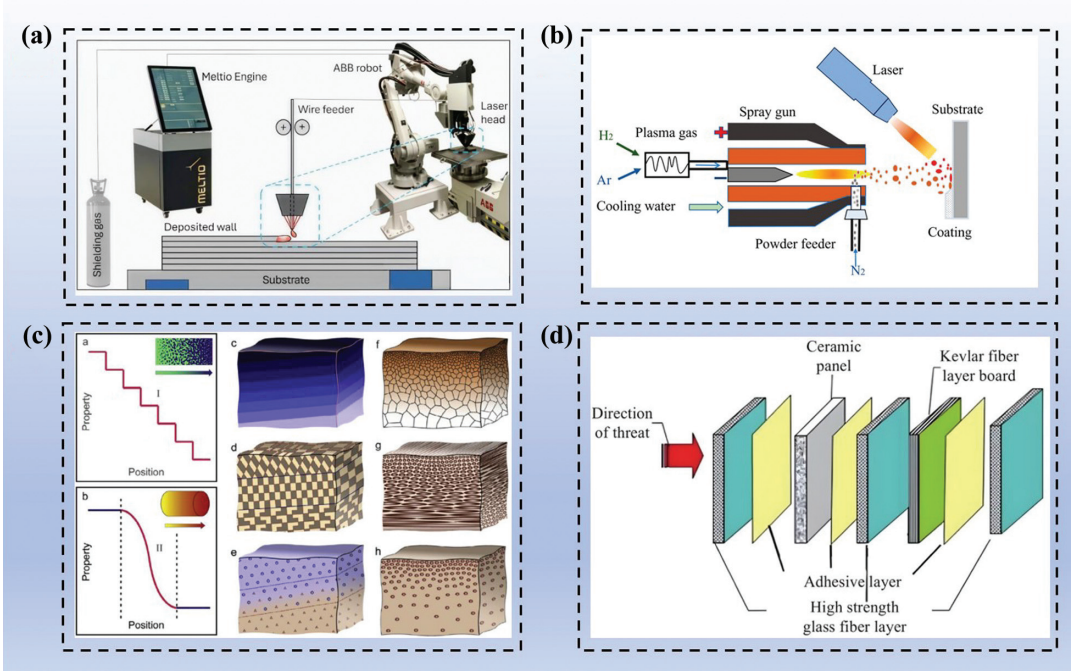

Fig. 4. Main research directions of advanced railway wheel materials: (a) and (b) surface modification and coating strengthening technologies, (c) manufacturing technologies for functionally graded materials (FGMs), and (d) layered/composite structural material technologies.

leading to a substantial reduction in wear of wheel–rail samples. Surface modification and coating technologies improve material performance by altering the substrate surface or depositing hard, wear-resistant phases, thereby improving surface hardness and wear resistance. Regarding gradient-structured materials, Zhao *et al.* [31] fabricated an Fe-based NbC gradient layer using hot-press sintering and in situ reaction techniques. The resulting structure presented micro-scale/nanoscale gradient characteristics: a surface layer rich in micro-/nanosized NbC particles and a subsurface NbC-Fe gradient region. Such a design integrates ceramic reinforcement and gradient toughening mechanisms, alleviating the common strength–toughness trade-off in ceramic–metal composites. Bai *et al.* [32] fabricated a dense TiC-Fe gradient coating on cast iron using a two-step in situ reaction method. The coating showed a gradient decrease in hardness and elastic modulus from the surface to the interface, accompanied by a gradient increase in fracture toughness. Gradient structures mitigate interfacial mismatch between hard phases and the matrix, enabling improved hardness without sacrificing overall toughness. For layered and composite structures, Sadeghi *et al.* [33] produced a laminated composite consisting of one magnesium alloy layer and two stainless steel layers via reactive transient liquid phase bonding, achieving both high specific strength and ductility. Kang *et al.* [34] fabricated a laminated structure using rolling bonding and high-pressure torsion, composed of TWIP steel sandwiched between two IF steel layers (IF-TWIP-IF), demonstrating high surface strength, hardness, and excellent ductility. Wu *et al.* [35] developed TiBw/Ti composites with various heterogeneous architectures, including quasi-continuous network, dual-scale network, layered-network hybrid, and 3D interconnected reinforcement structures, achieving a ~5-fold increase in plasticity compared with pure titanium. The synergistic deformation mechanisms in layered composites improve the strength–ductility balance.

In summary, existing studies show that rational structural design, combined with advanced fabrication processes involving gradient, multilayer, and surface engineered architectures in metallic materials, can improve key mechanical properties, including strength, hardness, toughness, and wear resistance. A comparative evaluation of these advanced strengthening and manufacturing technologies is provided in Table II. Such strategies are effective in mitigating the intrinsic conflict between strength and toughness, while also promoting stronger interfacial bonding between coating and substrate and improving overall service performance. These findings provide an important theoretical basis and technical framework for the development of high-performance metal-based composites intended for severe operating conditions. In view of such advantages, considerable potential exists for the future application of such materials in railway wheel manufacturing and the improvement of long-term service durability.

B. WHEEL GEOMETRY, PROFILE DESIGN, AND CONTACT CONTROL

Wheel wear resistance is determined not only by material properties but also by geometric design and key structural parameters. Wheel geometry sets the wheel–rail contact conditions and therefore affects vehicle dynamics, including stability and curving behavior. Wear then modifies tread and flange geometry during service, leading to progressive change in contact geometry, contact stress distribution, and the resulting wear and fatigue response. Given the scale of railway networks and the cost of rail renewal, wheel profile design and reprofiling practice often provide a more practical and economical route for managing wheel–rail contact conditions than altering rail profiles.

Table II. Comparative evaluation of advanced material strengthening and manufacturing technologies

Technology type	Cost	Performance improvement mechanism	Key issues	Application areas	Overall evaluation
Surface modification and coating strengthening technologies	Low	Improves surface properties (wear, corrosion, fatigue resistance)	Interface failure (delamination, cracking), limited thickness	Tools, bearings, molds, aerospace components	Most mature and cost-effective
Manufacturing technologies for functionally graded materials (FGMs)	High	Continuous gradient in composition and properties	Complex manufacturing, high cost, limited standardization	Aerospace, thermal barrier coatings, nuclear engineering	High potential for advanced applications
Layered/composite structural material technologies	Medium–high	Combines different materials for synergistic properties	Delamination, interface reliability, anisotropy	Aerospace structures, armor materials, lightweight design	Highly designable but interface-sensitive

1). TREAD PROFILE DESIGN AND OPTIMIZATION METHODS. Compared with the lengthy development cycle and relatively difficult experimental validation of wheel materials, optimizing wheel structural parameters under constant material conditions represents a more feasible approach for improving wheel wear performance. Therefore, various wheel profile optimization methods have been proposed, and their main categories are summarized in Fig. 5.

(1) Wheel profile optimization based on wheel–rail geometric contact characteristics
Shevtsov *et al.* [36] proposed a wheel profile design framework based on wheel–rail geometric contact characteristics. This approach employs numerical optimization techniques and adopts a response surface method based on multipoint approximation to minimize the deviation between the target rolling radius difference (RRD) function and the actual RRD function. Cui *et al.* [37] proposed a forward optimization method for wheel profiles based on the weighted normal gap at wheel–rail contact points. Taking the wheel–rail combination of an LMA wheel profile and a CHN60 rail as an example, the optimized profile improved the distribution of contact points and reduced wheel–rail forces. Santamaria *et al.* [38] optimized wheel profiles based on an ideal equivalent conicity curve, achieving a more uniform distribution of contact points within the effective contact region, thereby reducing contact stress and improving wear performance. Yao *et al.* [39] used the dispersion of equivalent conicity for wheel profiles matched with CN60 and CN60N rails as the optimization objective. By applying the fast non-dominated sorting genetic algorithm (NSGA-II), the lateral positions of arc centers near the rolling circle were improved. The optimized profiles reduced equivalent conicity dispersion and improved adaptability to different rail profiles and track conditions.

(2) Wheel profile optimization based on vehicle dynamic performance
Cui *et al.* [40] proposed a multi-objective optimization method aimed at reducing lateral wheelset forces and retaining running stability, thereby defining geometric design requirements for wheel profiles. Particle swarm optimization (PSO) was used to obtain a tread profile that satisfies operational safety requirements. Fu [41] applied a multi-population genetic algorithm (GA) to optimize wheel profiles for freight trains under acceleration conditions, using comprehensive vehicle dynamic parameters as design objectives. The study investigated the matching performance between equivalent conicity and vehicle/track parameters, identifying the optimal equivalent conicity as a constraint. The optimized profiles improved both dynamic performance and wear behavior. Hou *et al.* [42] optimized wheel profiles based on the original LMA profile using a Gaussian function correction (GFC) method combined with a Kriging surrogate model (KSM). This method mainly modifies the flange root region to improve curving performance and reduce wheel wear.

(3) Wheel profile optimization based on wear performance
Choi *et al.* [43] optimized the wheel flange profile using the NSGA-II algorithm with the objective of reducing flange wear and surface fatigue. The optimized profile demonstrated improved performance, with reduced flange wear and fatigue damage. Pacheco *et al.* [44] proposed a wheel profile optimization method considering both RCF and wear performance. Using NSGA-II, three optimized profiles were obtained with reduced wear indices and substantially improved fatigue indices. Lu *et al.* [45] established a nonlinear numerical optimization model for wheel profiles based on a backpropagation (BP) neural network, with wheel arc parameters as input variables and circumferential tread wear rate as the objective function. A single-objective, multi-variable, multi-constraint optimization approach was employed to minimize tread wear rate. Firlik *et al.* [46] proposed a biologically inspired black-box optimization algorithm (BBOA) for tread profile optimization. The optimized profiles showed improved wear indices and derailment coefficients compared with currently used profiles.

In summary, wheel profile optimization has become an important means of improving wheel–rail interaction and extending wheel service life. Optimization methods based on geometric contact characteristics offer advantages in computational efficiency and modeling simplicity but often cannot reflect vehicle dynamic behavior under actual operating conditions. By contrast, methods based on vehicle dynamic performance can provide a more comprehensive assessment of wheel–rail forces, running stability, and curving performance, although they impose higher demands on computational cost and model accuracy. In recent years, advances in artificial intelligence have promoted growing interest in intelligent multi-objective optimization, making it possible to achieve a better balance among wear, RCF, and vehicle dynamic performance. Future research is

therefore expected to move toward multidisciplinary coupled modeling, intelligent multi-objective optimization, and data-driven methods, with the aim of achieving coordinated optimization of overall wheel–rail system performance.

2). EQUIVALENT CONICITY AND WHEEL–RAIL CONTACT GEOMETRY. As train operating speeds continue to increase, wheel–rail interaction, as a fundamental issue in vehicle-track system dynamics, has become significant and has received sustained attention. Wheel–rail contact geometry lies at the core of wheel–rail interaction research. Among the relevant geometric parameters, equivalent conicity plays a particularly important role in supporting both the dynamic behavior of vehicles and the wear characteristics of the wheel–rail interface. Its magnitude directly influences the distribution of contact points and the associated contact stress level, making it a key parameter in wheel profile optimization. Appropriate control of equivalent conicity can reduce wear, prolong the service life of wheel–rail systems, and improve vehicle running safety and stability.

In terms of calculation and characterization methods for equivalent conicity, Gan [47] employed simplified, harmonic, and UIC519 methods to calculate the equivalent conicity of widely used domestic wheel profiles. A dedicated software tool for wheel–rail contact analysis was developed, and it was shown that the harmonic method and the UIC519 algorithm provide more accurate results. Qian *et al.* [48], based on the wavelength formula of wheelset hunting motion, used a method for calculating equivalent conicity in turnout regions. They also proposed a nominal equivalent conicity corresponding to the most probable lateral displacement of the wheelset to evaluate wheel–rail contact geometry in these regions. Damsongsaeng *et al.* [49] utilized a dual extended Kalman filter to estimate equivalent conicity in real time for condition monitoring and stability control. Xu and Dong [50], based on nonlinear wheel–rail contact theory, investigated the influence of nonlinear equivalent conicity on the running behavior of EMUs under conditions of identical nominal equivalent conicity. Their results showed that even with the same nominal value, significant differences in wheel–rail interaction may exist. Accordingly, a new evaluation approach was proposed in which statistical data were used to derive the nonlinear coefficient and nonlinear equivalent conicity over the range of 1 to 6 mm. Both field tests and numerical simulations showed that nominal equivalent conicity cannot accurately represent wear-related contact conditions, whereas the proposed indices, which combine nominal conicity with the slope of the conicity curve, can more effectively characterize the nonlinear features of wheel–rail contact. Regarding the relationship between equivalent conicity and vehicle dynamics, Kulkarni *et al.* [51] investigated the influence of wheel–rail contact conditions on vehicle dynamic performance using NP-$\lambda_3$mm (equivalent conicity at 3 mm lateral displacement) scatter plots derived from a conicity function database. The results indicated a negative correlation between $\lambda_3$mm and NP; higher $\lambda_3$mm values correspond to more negative NP values, which may reduce the nonlinear critical speed of the vehicle. Gerlici *et al.* [52] studied the matching behavior between different wheel profiles and rails and confirmed, through simulations, a significant correlation between equivalent conicity and critical speed. In terms of optimization design based on equivalent conicity, Chen *et al.* [53] used measured profiles of a 60D40 switch rail as optimization samples and obtained an optimized rail profile by inversely calculating from reduced equivalent conicity curves. This method, based on the relationship among equivalent conicity, RRD, and rail profile slope, improves ride stability when passing through turnouts and enables effective conicity optimization. Ersson *et al.* [54] proposed a new gradient index profile (GIP), which decomposes equivalent conicity into wheel and rail components, allowing independent constraints on wheel and rail profiles and enabling more precise prediction and control of equivalent conicity.

Overall, existing studies indicate that equivalent conicity, as a concise, practical, and widely used parameter for characterizing wheel–rail contact geometry, plays a pivotal role in wheel–rail profile design, dynamic performance assessment, and in-service condition monitoring. Its engineering application requires careful consideration of operating conditions, track and turnout geometry, and the nonlinear evolution of contact states during wear. On this basis, profile optimization guided by equivalent conicity, in combination with wheel–rail contact analysis and vehicle system dynamic simulations, remains an important approach for improving vehicle stability and wear performance.

C. MANUFACTURING PROCESSES AND HEAT TREATMENT

The increasingly severe demands imposed by heavy-haul service, high-speed operation, and harsh environmental conditions have made integrated control of forging, heat treatment, and property distribution a key issue in railway wheel design. Modern process design must satisfy not only the requirements for bulk strength and toughness but also the need for controlled rim hardness, stable near-surface behavior, and a favorable residual stress state. Against this background, wheel concepts based on dual hardness and hardness gradients have emerged as promising strategies for improving resistance to wear, RCF, and thermally induced surface damage.

1). FORGING AND HEAT TREATMENT, MICROSTRUCTURE, AND RESIDUAL STRESS. As a typical large load-bearing component, the service performance of railway wheels is governed by their microstructure and mechanical properties. Heat treatment serves as a core technological approach for tailoring microstructural features and property distributions. Through rational design of heat treatment routes, it is possible to achieve a synergistic improvement in wear resistance and RCF performance while maintaining overall wheel strength. As a results, optimization of heat treatment processes based on service requirements has become a key research focus in this field.

Tao *et al.* [55] proposed an improved quenching process integrating spray control with phase transformation characteristics. By introducing a holding stage at 700 °C for 600 s prior to conventional spray quenching, bainite transformation was promoted and its volume fraction increased. The results showed that the process reduced the performance gradient between the surface and core, improving the overall strength–toughness balance by around 20%. Zhang *et al.* [56] investigated the effect of annealing at 500 °C on pearlitic wheel steel and found that annealing relieved local residual stresses and reduced stress concentration, thereby

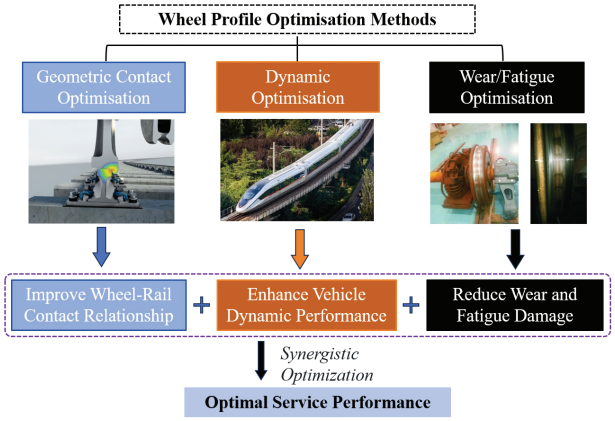

Fig. 5. Wheel profile optimization methods.

improving fracture toughness and fatigue performance. Gao *et al.* [57] optimized the quenching–tempering process by regulating bainitic ferrite content and retained austenite stability. By adopting a combined cooling path of water mist spraying and air cooling, proeutectoid ferrite precipitation was suppressed while bainite transformation was promoted, resulting in a synergistic improvement of strength and toughness. Liu *et al.* [58] conducted quenching–tempering experiments on CL60 wheel steel and revealed the influence of tempering temperature on microstructural evolution and wheel–rail matching performance. As the tempering temperature increased, the microstructure transformed from tempered troostite to tempered sorbite, accompanied by a gradual decrease in hardness. Meanwhile, the wheel–rail wear rate exhibited a trend of first increasing and then decreasing, with the highest wear corresponding to tempered sorbite. Zhang *et al.* [59] studied the effect of plasma quenching parameters on contact fatigue performance and found that martensite formation and residual compressive stress induced by rapid heating and cooling could increase fatigue life by approximately 30%. However, excessive local residual tensile stress may also trigger crack initiation and spalling failure. Wang *et al.* [60] proposed a composite process combining laminar plasma quenching and tempering, which reduces lattice distortion and optimizes microstructure, thereby suppressing RCF damage while maintaining wear resistance. Li *et al.* [61], based on high-throughput characterization techniques, used a quantitative method for analyzing the distribution of composition, microstructure, and hardness in wheel materials. The study revealed the gradient distribution of microstructure and properties from the tread surface to a depth of 50 mm and applied a statistical correlation between ferrite area fraction and microhardness. In addition, the application of finite element methods and intelligent algorithms enables rapid optimization of heat treatment parameters and multi-scheme comparison while reducing experimental costs, providing important support for intelligent heat treatment. Chen and Lingamanaik [62] analyzed the formation mechanism of residual stress during spray quenching using finite element methods, highlighting the significant influence of quenching time, spray position, and cooling configuration on temperature evolution and phase transformation behavior. Cuperus *et al.* [63] demonstrated through nonlinear finite element simulations that accurate prediction of residual stress requires comprehensive consideration of creep behavior, latent heat of phase transformation, transformation strain, and complex heat transfer boundary conditions. Tian *et al.* [64] developed a thermos-phase transformation coupled model, revealing the influence of asymmetric cooling on microstructural evolution and hardness distribution, and identifying spray angle as a key parameter for controlling temperature history and hardness uniformity. Furthermore, combined experimental and simulation analyses showed the nonuniformity of rim hardness distribution and clarified the influence of local hardening (or gradient hardness) on stress and wear behavior. Xiong *et al.* [65] evaluated five machine learning algorithms for predicting steel properties and found that random forest regression achieved the best predictive performance. Further research utilized the mapping relationship between tempering temperature and material properties using machine learning techniques.

Overall, existing studies indicate that optimization of quenching paths, control of cooling rates, and the introduction of multistage heat treatment strategies make it possible to achieve coordinated regulation of multiphase microstructures, including bainite, pearlite, and retained austenite, thereby improving the strength, toughness, and wear resistance of wheel materials. As shown in Fig. 6, research on wheel heat treatment has gradually progressed from traditional empirical process design to a more systematic framework centered on microstructural regulation, performance optimization, and intelligent prediction. At the same time, increasing attention has been directed toward the relationship between microstructural evolution and macroscopic properties, which has clarified the critical roles of hardness gradients, residual stress distribution, and microstructural features in wheel–rail service behavior. However, several limitations remain. Most existing studies focus on individual process parameters or localized microstructural control, while systematic optimization from a full life cycle perspective is still lacking. In addition, efficient coupling between experimental investigation and numerical simulation has yet to be achieved, particularly in the accurate prediction of multiphysics phase transformation behavior and residual stress evolution. Furthermore, the mechanisms by which heat treatment affects wheel–rail matching and service damage evolution remain insufficiently understood.

2). DUAL HARDNESS AND SURFACE HARDENING TECHNOLOGIES. Local hardening or dual-hardness treatment of railway wheels is commonly achieved through plasma quenching. Plasma quenching is a surface strengthening technique belonging to the category of thermal surface hardening. Its core principle involves rapid heating of the metal surface using high-temperature plasma energy, followed by rapid cooling through self-conduction of the workpiece, thereby inducing phase transformation in the surface layer (e.g., formation of high-hardness martensite). The process improves surface hardness, wear resistance, and fatigue strength while maintaining good toughness in the substrate. Isakaev *et al.* [66] developed a computer-controlled plasma surface strengthening technology capable of locally hardening the wheel tread and flange. The process increased surface hardness from approximately 255 HB to 420–450 HB, while improving wear resistance by 2–3 times and fatigue resistance by about 1.5 times. Kanaev *et al.* [67] systematically investigated the mechanisms and experimental results of plasma quenching, demonstrating that it forms a non-equilibrium surface layer on the wheel

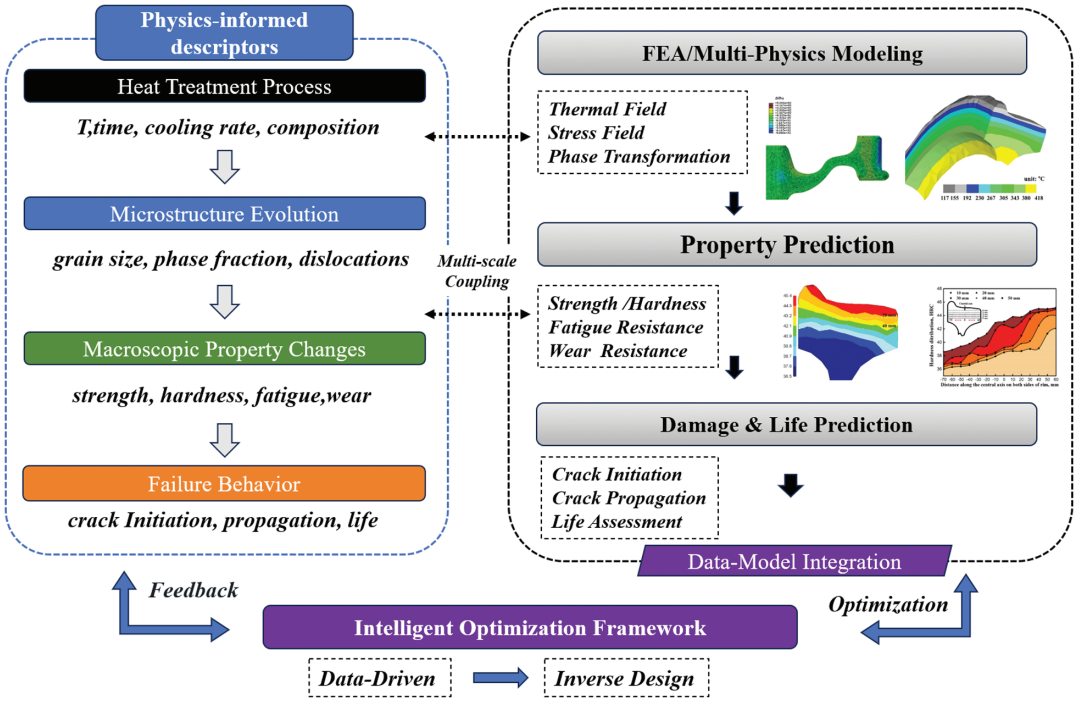

Fig. 6. Framework of coupling mechanism between wheel heat treatment process, microstructure evolution, property response, and finite element intelligent optimization [62].

flange and rim, thereby improving surface hardness and wear resistance. Yusupov *et al.* [68] conducted comparative experiments between plasma-quenched and untreated freight car wheels and successfully applied this technology to locomotive and passenger wheels, improving flange wear resistance and extending service life. In recent years, with the successful application of kilowatt-level fiber lasers, laser heat treatment has emerged as an advanced alternative. Compared with plasma quenching, laser heat treatment offers several advantages, including low strain and stress levels, high scanning speed, capability for deep processing, and low maintenance cost. As a results laser-based processes are gradually replacing plasma quenching in practical applications. Bogdanov *et al.* [69] compared laser quenching and plasma quenching techniques for improving wheel tread strength and contact fatigue resistance and determined the optimal process parameters for laser heat treatment of wheel steel, achieving superior surface wear resistance. Gubenko *et al.* [70] proposed a method to improve tread wear resistance via localized laser treatment and analyzed the effects of pulsed and continuous laser modes on the microstructure and properties of wheel steel. Their results confirmed that laser processing effectively improves surface hardness and wear resistance. Cao *et al.* [71] investigated the microstructure, wear performance, and RCF behavior of wheel–rail materials after laser dispersed quenching. The results showed that the treated regions exhibited a uniform martensitic structure with increased surface hardness, thereby improving wear resistance. Fayzibaev *et al.* [72] proposed a method to calculate the depth of the strengthened layer on wheel rolling surfaces. By applying controlled impact forces using a dedicated impact device, plastic deformation is induced in the flange surface layer, thereby increasing surface hardness. Gubenko *et al.* [73] compared wheel steel subjected to induction thermal cycling with untreated material and found that the formation of sorbite structures and associated compressive stresses improved fatigue resistance.

In summary, local hardening and dual hardness wheel structures are achieved through surface heat treatment technologies, which rely on regulating near-surface microstructures to balance wear resistance and fatigue performance. Plasma quenching can increase surface hardness and improve wear resistance and has already been widely adopted in engineering practice. However, the non-uniform residual stress state introduced by such treatment may increase the risk of fatigue damage. By contrast, laser heat treatment, owing to its controllable energy input and reduced thermal effect, shows greater potential for optimizing microstructure and residual stress distribution and is emerging as a major development direction. At the same time, methods such as impact strengthening and induction thermal cycling reflect a broader trend toward multi-process synergistic improvement. Despite such progress, significant challenges remain in understanding the multiscale coupled mechanisms governing dual hardness wheels and in predicting their long-term service performance, indicating a continued need for more precise control and intelligent optimization.

D. ENVIRONMENTAL DURABILITY AND SERVICE CONDITIONS

As railway systems extend across broader geographic regions and operate under increasingly demanding conditions, environmental adaptability has emerged as an important issue in railway wheel design. Wheels are required to withstand not only RCF, wear, impact, and thermal loading but also environmental exposure associated with low temperature, humidity, salinity, and contamination. Such factors can alter material response and damage evolution, particularly in relation to embrittlement and corrosion-

related deterioration, thereby affecting the stability and durability of wheel service performance. A clear understanding of environmental effects is therefore essential for the development of wheel materials and designs suitable for different operating regions and service conditions.

1). LOW TEMPERATURE SERVICE, EMBRITTLEMENT, AND DAMAGE MECHANISMS. Existing studies indicate that low-temperature environments affect wheel service performance mainly through three aspects: adhesion behavior, plastic deformation, and material toughness. Shi *et al.* [74] reported that under dry conditions, low temperatures suppress surface oxidation on the wheel, thereby increasing the adhesion coefficient. However, under both ambient and low-temperature conditions, the presence of water, oil contaminants, or antifreeze reduces the adhesion coefficient to low levels, and low temperatures prolong the adhesion recovery process under water-mediated conditions. Zhou *et al.* [75] found through wheel–rail experiments that decreasing temperature can reduce wheel wear due to the formation of a wear debris layer. However, both increases and decreases in ambient temperature can aggravate rail wear. Furthermore, decreasing temperature intensifies plastic deformation and work hardening on the wheel–rail contact surface. At −40 °C, a WEL induced by severe plastic deformation was observed on the wheel surface. Although this layer increases surface hardness, it reduces material toughness, making the material more prone to brittle fracture and spalling.

Ostash *et al.* [76] demonstrated that medium- to high-strength railway wheel steels containing fatigue crack-like defects exhibit low-temperature embrittlement (down to −60 °C) under high cyclic loading amplitudes, particularly when the fatigue crack growth rate exceeds 10^{-7} m/cycle. Li *et al.* [77] reported that, under both dry conditions and with the use of friction modifiers, temperature variation does not affect the degree of wheel fatigue damage. In all temperature conditions, friction modifiers can reduce wheel wear rates while maintaining relatively mild RCF damage; however, under low-temperature conditions, rail wear may be aggravated. These results indicate that the proper use of friction modifiers plays a positive role in improving wheel performance in low-temperature environments. Liang *et al.* [78] introduced nanoscale tungsten carbide (WC) particles under low tempering temperatures, achieving a synergistic effect of reduced lattice distortion in bainitic ferrite, precipitation strengthening, and improved toughness, while maintaining the content and stability of retained austenite. The process improved the overall mechanical properties of the steel by 17% and increased impact toughness by 41%, thereby improving wheel service performance. In summary, for cold region applications, the use of high toughness wheel steels, together with appropriate friction modification strategies, can improve wheel service performance.

2). HOT HUMID SERVICE, CORROSION, ADHESION, AND WEAR. Railway wheels operate under long-term exposure to open environments, where humid and hot conditions affect their service performance by altering interfacial chemical reactions and wear mechanisms at the wheel–rail contact. Rong *et al.* [79] investigated the influence of environmental humidity on adhesion characteristics and damage behavior at the wheel–rail interface under different weather conditions. The results showed that humidity has a pronounced effect on adhesion behavior. Under low-humidity conditions, fatigue wear dominates; as humidity increases, abrasive wear becomes more severe, since oxide debris acts as abrasive particles and accelerates wear. Under high-humidity conditions, a friction-reducing layer forms, which protects the rolling surface from excessive wear. However, such environments are unfavorable for safe railway operation, as high temperature and humidity promote the formation of tribochemical products (a mixture of iron oxides and water molecules), leading to a significant reduction in the adhesion coefficient between wheel and rail. He *et al.* [80] studied the effects of environmental humidity on the adhesion characteristics and damage behavior of CL60 wheel steel. Their results indicated that under high-humidity conditions, the degree of surface oxidation increases with temperature. The formation of iron hydroxides increases friction and accelerates surface damage. With increasing relative humidity, water content in oxide debris reaches saturation, causing the debris to become paste-like, which reduces the adhesion coefficient. Moreover, under high humidity, the plastic deformation layer on the wheel surface becomes thicker, and both the depth and length of cracks exceed those observed under medium and low humidity conditions. Li *et al.* [81] selected widely used 316L and 420 stainless steel alloy powders as cladding materials and designed three environmental conditions based on temperature and humidity variations across different regions in China (25 °C-60% RH, 50 °C-60% RH, and 50 °C-90% RH). Through friction and wear tests, they evaluated the performance of wheels repaired by laser cladding under these conditions. The results demonstrated that wheels repaired using 316L stainless steel powder exhibited superior tribological performance.

Overall, current studies have identified the key mechanisms governing wheel material behavior in low-temperature environments, particularly the coupled effects of adhesion behavior, plastic deformation, microstructural evolution, and brittle fracture. Despite such progress, a systematic understanding of multivariable coupling and long-term service behavior under extreme low-temperature conditions remains insufficient. In hot and humid environments, degradation is dominated by tribochemical effects, but existing research still focuses on isolated environmental factors. As a result, the coupled influences of multiple fields and the long-term evolution of corrosion and fatigue damage remain inadequately understood.

III. IN-SERVICE DEGRADATION AND LIFE PREDICTION

Wheel–rail contact governs the transfer of traction and braking forces, wheelset guidance, and the dynamic stability margin of railway vehicles, making it a core issue in railway safety and durability. Wear and surface damage at the wheel–rail interface are not only material degradation problems but also manifestations of evolving contact mechanics under repeated rolling, creepage, impact, and changing profile geometry. Over many years, rig-based and full-scale tests have been widely used to investigate whether higher wheel and rail hardness can mitigate rapid wear and delay surface-initiated damage and to determine how wheel–rail hardness matching affects service life at the system level. When wear becomes severe, or when spalling and polygonal wear develop, deterioration in ride quality, increased vibration and impact loading, and accelerated damage to both wheels and rails may follow. Accurate

prediction of wear and profile evolution is therefore a prerequisite for effective reprofiling and renewal decisions and is central to wheelset life extension, life cycle cost reduction, and the maintenance of stable operating quality.

A. WHEEL–RAIL MATERIAL MATCHING, HARDNESS RATIO, AND WEAR RESPONSE

To improve wheel–rail wear performance and to clarify the effect of material pairing on wheel wear resistance, extensive experimental investigations have been carried out using wheel–rail test rigs, as shown in Fig. 7. These studies indicate that the wheel–rail hardness ratio has a significant influence on the wear behavior of both wheels and rails, with localized fatigue-related wear generally emerging as the dominant damage mode. Maintaining the hardness ratio within an appropriate range is therefore essential for optimizing wheel–rail wear performance and ensuring safe train operation.

Conventional studies held that increasing the hardness of one material reduces its own wear but aggravates the wear of the mating material [82,83], indicating a typical trade-off in wheel–rail wear. However, full-scale tests conducted by Stock *et al.* [84] and Heyder *et al.* [85] showed that increasing rail hardness did not increase wheel wear; under some matching conditions, wheel wear even decreased. Zhao *et al.* [86] studied similar findings, namely that increasing rail hardness reduced rail wear, while wheel wear changed only slightly. To explain these discrepancies, researchers proposed that the wheel–rail hardness ratio may be the key parameter governing wear behavior and subsequently carried out systematic studies to reveal its regulatory mechanism. Hu *et al.* [87] investigated multiple cross-matched combinations of wheel and rail materials and found that wheel wear rate decreases with increasing wheel hardness. Under certain creepage and contact-pressure conditions, rail wear was also correlated with wheel hardness. Meanwhile, the overall wear rates of the wheel–rail system increased with increasing wheel/rail hardness ratio, indicating that hardness matching has a pronounced effect on wear behavior. Wang *et al.* [88] showed that, with increasing wheel hardness, wheel wear decreases whereas rail wear increases, and the total wheel–rail wear first decreases and then increases, reaching a minimum when the wheel and rail hardness are approximately matched. At the same time, the dominant damage mode shifts from pitting and spalling at lower hardness to large-scale spalling at higher hardness, while rail damage evolves from slight spalling to deeper subsurface spalling. These results further indicate that, as the wheel/rail hardness ratio increases, wheel wear decreases and rail wear increases, and that the total wear reaches an optimum when the hardnesses are properly matched. It provides a quantitative basis for understanding the influence of hardness ratio on wear partitioning and service performance. Hu *et al.* [89] further investigated the effects of varying wheel–rail hardness ratio on wear and RCF behavior. Their results showed that when the wheel/rail hardness ratio (Hw/Hr) increased from 0.927 to 1.218, the wheel wear rate decreased, with the most pronounced reduction occurring at Hw/Hr = 1.218, whereas the rail wear rate increased. Zhang *et al.* [90] studied wheel–rail pairs with different hardness levels and found that when the wheel/rail hardness ratio was controlled at approximately 1.15:1, the total wear was minimized and the surface damage was the least severe. Increasing wheel hardness reduced wheel wear and suppressed polygonal wear. Chang *et al.* [91] evaluated nine hardness-matching combinations involving three types of wheel and rail materials. It found that when the wheel/rail hardness ratio was below 1.05, polygonal wear readily developed on the wheel specimens, whereas when it exceeded 1.36, polygonal wear was almost completely suppressed, although rail wear increased. The results indicate that the wheel–rail hardness ratio plays a decisive role in regulating wear partitioning. Ma *et al.* [92] evaluated the wear behavior of six rail materials paired with wheel specimens of different hardness and analyzed wear debris morphology, microhardness, and contact fatigue performance. The results showed that when the rail/wheel hardness ratio (Hr/Hw) was below 0.96, rail wear increased; when Hr/Hw exceeded 1, the rail wear rate remained at a relatively low level, and when Hr/Hw exceeded 1.25, rail wear decreased sharply. In contrast, wheel wear shown that the opposite trend, increasing when Hr/Hw reached 1.28.

Overall, current studies indicate that maintaining the wheel–rail hardness ratio within approximately 1.0 to 1.2 is beneficial for reducing wear and mitigating damage, thereby improving the overall service performance of the wheel–rail system. Control of the wheel–rail hardness ratio has thus become a key approach to improving wear resistance and service reliability. However, although the basic relationships among hardness ratio, wear partition, and damage evolution have been built, the coupled influences of contact stress, creepage, and material microstructure under complex operating conditions remain to be clarified. Addressing these issues will be essential for translating current understanding into practical wheel–rail design and maintenance strategies.

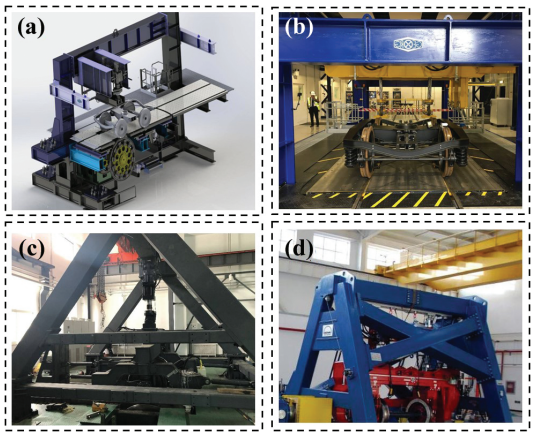

Fig. 7. Wheel–rail interaction test rig.

B. WHEEL WEAR PREDICTION AND PROFILE EVOLUTION

Wheel wear prediction is generally formulated as a profile evolution problem for the tread and flange under representative operating conditions. In a typical simulation framework, a virtual operating environment is first designed by specifying route geometry and irregularities, vehicle speed history, traction and braking conditions, wheel–rail contact states, and material properties. The vehicle-track system response is then computed to obtain contact forces, creepages, and contact patch kinematics, which are

subsequently linked to a wear law to estimate local material removal and update the wheel profile over a reprofiling interval. Most mechanism-based approaches are therefore built on the coupling of three essential modules, namely a vehicle-track dynamic model, a wheel–rail contact model for normal and tangential interaction, and a wear calculation module with profile updating and smoothing procedures. In parallel, data-driven approaches have been developed from measured profile histories and wear-related indicators using numerical analysis, regression methods, and machine learning techniques. Such approaches are increasingly used to accelerate prediction, improve computational efficiency, and compensate for model bias associated with fleet variability and operational uncertainty.

1). MECHANISM-BASED WEAR MODELING. Numerous physical-driven models have been developed for wheel wear prediction. Pearce and Sherratt [93] proposed a simplified cyclic calculation model in which the wear distribution along the wheel profile is predicted by accumulating wheel–rail contact positions, creep forces, and creepages. Bevan *et al.* [94] developed a damage model based on route operating spectra, in which parameters such as curve radius, cant, and traction/braking conditions were incorporated into dynamic simulations to achieve coupled prediction of tread wear and RCF. Wang *et al.* [95] used an integrated model coupling wheel wear with vehicle dynamics. By considering nonlinear factors in the traction transmission system, the model was able to analyze the wear differences between motor and trailer cars, and its accuracy was validated against field measurements. Chang *et al.* [96] constructed a three-dimensional dynamic finite element model in Abaqus and combined it with the Archard wear law to predict wheel–rail rolling contact wear. Zeng *et al.* [97] coupled a vehicle dynamics model with the Archard model to reveal the evolution of wheel wear under acceleration conditions. Braghin *et al.* [98] combined multibody dynamics with the FASTSIM algorithm, achieving relatively high accuracy in tread wear prediction. To assess the applicability of different modeling approaches, many comparative studies have also been carried out. Wang [99] analyzed several signal processing methods and pointed out that Fourier transform and moving average methods are more advantageous for polygonal wear prediction. Niu *et al.* [100] compared Hertzian and semi-Hertzian contact algorithms and found that the semi-Hertzian model is closer to actual behavior in long-term wear prediction. Further studies have shown that different contact models can influence prediction results. Tao *et al.* [101] reported that the Hertz + FASTSIM combination provides a good balance between computational efficiency and accuracy. Yang *et al.* [102] showed that non-Hertzian models offer higher accuracy but at greater computational cost, whereas Hertzian models are more suitable for long-term engineering applications of wear prediction. Overall, physical wheel wear prediction models have evolved from simplified empirical formulations to refined multiphysics coupled models.

Current studies show that mechanism-based wear prediction can reproduce tread and flange profile evolution when route spectrum, operating states, contact algorithms, and profile update rules are specified consistently, and validation against twin-disk or field measurements is essential to demonstrate credibility. The key risk is that long-distance prediction is sensitive to modeling choices that are often treated as technical details, including contact formulation (Hertz versus non-Hertz), tangential algorithm, smoothing strategy, and the representation of traction, braking, and variable friction; these choices can shift predicted wear migration and flange involvement. Mechanism-based workflows can therefore be configured around the intended application, using computationally efficient contact models for fleet-level studies when justified, and reserving higher-fidelity contact or FE formulations for regimes where stress distribution, plasticity, and local damage mechanisms govern wear evolution.

2). DATA-DRIVEN WEAR MODELING. To address the limitations of conventional vehicle-dynamics-based models, particularly their high computational cost and limited generalizability, researchers have turned to data-driven approaches for wheel wear prediction. Early methods mainly relied on statistical models to fit and extrapolate historical data. Zhu *et al.* [103] employed polynomial functions based on operational data to predict wheel wear, while Costa *et al.* [104] combined inspection data with a Markov decision process (MDP) to construct prediction models for wear rate and service life. Although these methods are straightforward to implement, they are highly dependent on data quality and quantity, provide limited insight into complex underlying mechanisms, and often show insufficient long-term predictive accuracy. On this basis, machine-learning-based methods were gradually introduced. Chi *et al.* [105] employed a Bayesian model to predict polygonal wear, improving model flexibility, although the approach remained constrained by data scale and generalization capability. Iwnicki [106] developed a neural-network-based model with exogenous inputs for wheel–rail wear prediction. Deng *et al.* [107] combined a nonlinear autoregressive neural network with exogenous inputs (NARNN), the Levenberg-Marquardt (LM) algorithm, and orthogonal matching pursuit (OMP), improving both prediction accuracy and model compactness. In recent years, deep learning and data augmentation techniques have further advanced this field. Shangguan *et al.* [108] used TimeGAN to generate wear data and combined it with a gated recurrent unit (GRU) network for state prediction, alleviating the problem of insufficient data. Liu *et al.* [109] proposed a two-step prediction framework based on DBSCAN and multi-model fusion, enabling coordinated prediction of both fleet-level and single-wheel wear. In this framework, the GA-BPNN and LSTM models achieved the best performance in overall and individual prediction tasks, respectively.

Existing work indicates that data-driven methods can deliver rapid wear prediction and capture fleet variability when trained on representative inspection and monitoring datasets. Nevertheless, their generalizability may deteriorate when operating regimes, friction conditions, or maintenance practices differ from those represented in the training data. In addition, sensitivity to data quality, measurement consistency, and latent covariates can introduce prediction drift and confident remaining life estimates. Data-driven wear prediction is therefore most credible when operating state descriptors are incorporated, predictive uncertainty is quantified, and model calibration is constrained by physics-based knowledge.

3). HYBRID FRAMEWORKS FOR WEAR AND RCF PREDICTION. Both mechanism-based and data-driven approaches show clear limitations when used independently. Mechanism-based models are often

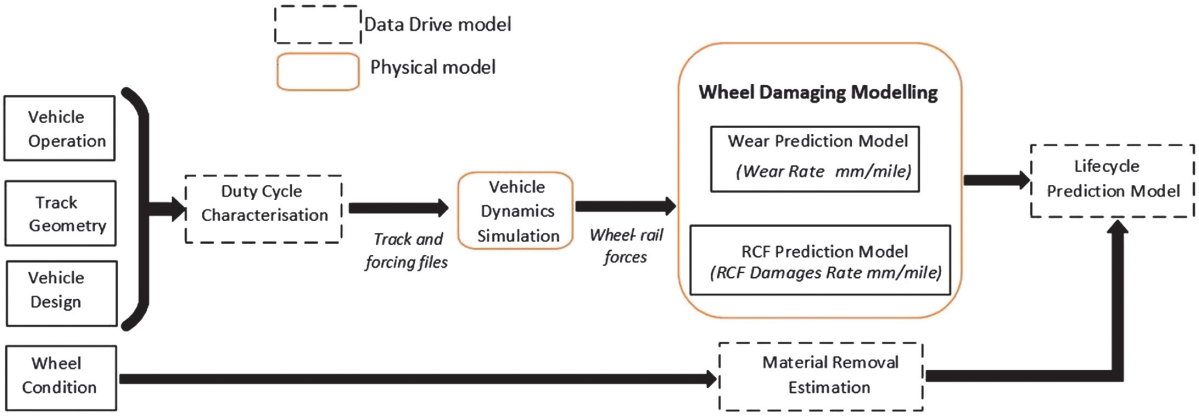

Fig. 8. Hybrid framework based on physics and data-driven models.

demanding and sensitive to the selection of contact algorithms and wear coefficients, whereas purely data-driven models may have limited transferability across routes and operating regimes and often lack physical interpretability. For this reason, hybrid frameworks have been proposed to combine physics-based structure with data-driven calibration or correction, as shown in Fig. 8, with the aim of improving prediction robustness and capturing the closed-loop evolution of wheel wear over successive reprofiling cycles.

Zeng *et al.* [125] introduced a physics-data dual-driven framework that couples wear evolution with reprofiling by integrating multi-location wear characteristics and reprofiling behavior within a closed-loop model. Numerical prediction was used to estimate wear state and assess remaining useful life (RUL), and the framework was reported to provide reliable prediction accuracy with practical application in wheel wear prediction and health management. Wang *et al.* [126] proposed a hybrid strategy in which a physics-based model first estimates degradation rates under representative operating conditions, and a data-driven model then evaluates wheelset life cycle using reprofiling removal at the flange, predicted or measured wear indicators, and operational reprofiling requirements. Outputs were used to determine maximum service life under safety regulations and operator performance criteria, with reported agreement against operational data from high-speed services. Zhu *et al.* [127] proposed a combined physical model and data-driven method that uses least squares regression to quantify discrepancies between measured and simulated wear at fixed mileage intervals and to calibrate the Jendel wear model. By integrating vehicle dynamics, wheel–rail contact modeling, and the calibrated wear model, metro wheel wear was predicted over additional mileage; improved accuracy and reduced dependence on empirically chosen wear coefficients were reported. Hartwich *et al.* [128] proposed a hybrid concept for wheel profile prediction that combines a dynamics model based on wheel–rail contact theory with postprocessing of measurement data.

Hybrid methods also motivate practical criteria for coordinating wear and RCF risk within maintenance decisions. When prediction outputs are used to schedule reprofiling, the relevant decision variable is not wear depth alone but also the combined evolution of profile geometry (affecting equivalent conicity and dynamics response) and damage accumulation (affecting RCF risk). Hybrid frameworks that embed reprofiling cycles therefore provide a natural route to define consistent intervention thresholds and to update remaining-life estimates as measured profiles and condition indicators become available.

The literature indicates that hybrid frameworks improve wear prediction credibility by calibrating wear coefficients and operating-state dependence against measurement data while retaining physics-based structure for extrapolation across mileage and reprofiling cycles. The key risk is that calibration can compensate for unmodeled mechanisms, such as friction variability, thermal history, and damage-mode transitions between wear and RCF, which can reduce robustness when conditions change. Hybrid prediction can therefore be implemented within a closed-loop maintenance framework in which operating descriptors, monitoring indicators, and intervention rules are aligned, and where model updating and uncertainty treatment are explicit.

Physics-based models are well suited for elucidating wheel–rail contact mechanisms and conducting parametric sensitivity analyses; however, the engineering deployment requires careful consideration of computational cost and parameter availability. Data-driven models, by contrast, are advantageous for online updating and rapid prediction, although their transferability across different lines and robustness under operating condition drift necessitate appropriate calibration strategies. Hybrid approaches that combine physics-based and data-driven paradigms are more suitable for closed-loop maintenance scenarios, where physical constraints can be leveraged to improve generalization capability, while data assimilation can be employed to mitigate long-term prediction bias.

Physics-based models are well suited for elucidating wheel–rail contact mechanisms and conducting parametric sensitivity analyses; however, their engineering deployment requires careful consideration of computational cost and parameter availability. Data-driven models, by contrast, are advantageous for online updating and rapid prediction, although their transferability across different lines and robustness under operating condition drift necessitate appropriate calibration strategies. Hybrid approaches that combine physics-based and data-driven paradigms are more suitable for closed-loop maintenance scenarios, where physical constraints can be leveraged to improve generalization capability, while data assimilation can be employed to mitigate long-term prediction bias.

Table III. Comparison of representative modeling approaches for wheel–rail wear and RCF assessment

Domain	Method type	Key inputs/data requirements	Key outputs/ indicators	Main features and applicability boundaries
Wear	Physics-based	Contact parameters, creepage, material properties, and operating conditions	Wear amount, profile evolution	High interpretability; sensitive to input parameters and computationally expensive; suitable for mechanism investigation and comparative assessment of schemes
Wear	Data-driven	Historical inspection data, operational data, and extracted features	Wear/life trends, RUL	Easy to update online; subject to transferability limitations and condition-drift risks; suitable for lines with sufficient data
Wear	Hybrid physics–data-driven	Physics-based prior constraints combined with data updating	Wear/RUL with uncertainty	Balances predictive accuracy and interpretability; complex framework construction; suitable for closed-loop operation and maintenance
RCF	Shakedown map/fatigue index	Contact stress and material parameters	Risk zoning/ thresholds, FI, etc.	Intuitive classification; limited capability in describing damage evolution and coupling effects; suitable for preliminary screening and early warning
RCF	Damage function/accumulation model	Creepage, load spectrum, and calibration parameters	Damage accumulation/ risk	Convenient for coupling with wear models; dependent on calibration quality; suitable for line-level assessment
RCF	Experimentally calibrated model	Experimental data, material parameters, and process parameters	Life/crack-related parameters	Effective for comparing materials and manufacturing processes; limited extrapolation capability; suitable for process validation

C. RCF ASSESSMENT UNDER WHEEL–RAIL LOADING

With the transition of wheel–rail systems from wear-dominated behavior to coupled multi-damage mechanisms, RUL assessment has become considerably more complex. International research has therefore placed increasing emphasis on RCF crack propagation, the competing effects of wear and spalling, and probabilistic RUL prediction. As a result, an integrated assessment framework combining physics-based models with statistical methods has gradually been developed. Johnson investigated RCF damage under both point and line contact conditions and proposed corresponding shakedown map criteria [115,116], which have become one of the most widely used core methods for predicting wheel RCF. Johnson [117] initially developed the shakedown map based on full sliding conditions, which was later extended to rolling–sliding conditions by Bower *et al.* [118]. This method qualitatively describes and evaluates the material response of wheel–rail systems under three parameters: maximum contact stress P_0, material shear yield strength k, and friction coefficient μ. Within the shakedown map framework, the horizontal shortest distance from the operating point to the ratcheting boundary is defined as the fatigue index (FI) for wheel–rail surface crack prediction. This FI is related to the initiation and propagation of surface fatigue cracks and is closely associated with spalling and flaking processes, which constitute severe and sudden wear mechanisms. A series of twin-disk experimental data indicate that, regardless of variations in normal load, the wear rate shows an exponential relationship with the fatigue index. Furthermore, when the FI approaches zero, it signifies the onset of severe wear. Some researchers have proposed that the fatigue index, derived from shakedown theory and used to predict surface-initiated fatigue in railway wheels, can serve as a key parameter for evaluating rolling contact wear rate [119]. However, other studies have shown that under high creepage conditions, the predictive capability of the FI for fatigue damage decreases [120]. Analysis based solely on the shakedown map has inherent limitations, as it does not account for the influence of material wear on RCF during rolling friction processes. Therefore, in addition to shakedown theory, it is necessary to combine other predictive approaches, such as damage functions, to systematically investigate fatigue damage behavior. Rolling contact simulation experiments have introduced the concept of dissipated energy per unit contact area, $T\gamma/A$, which has been shown to correlate with wear rate per unit length or contact area [121]. Based on this finding, new damage function models have been developed for wheel fatigue damage and wear, enabling the prediction of both fatigue crack propagation and wear rate. Butini *et al.* [122] developed a coupled model integrating wear and RCF, allowing simultaneous prediction of wheel–rail profile evolution and the accumulation of surface RCF damage. Dong [123] conducted thermo-mechanical coupled simulations to analyze the stress evolution of wheel treads during emergency braking of heavy-haul trains and predicted fatigue crack initiation life under different axle loads and brake shoe pressures. Mazzù and Donzella [124] proposed a predictive model based on steady-state strain fields derived from integral equations, considering shear stress and plastic strain increments along the depth direction, which can predict crack morphology under high-cycle loading conditions. Zhou *et al.* [125] developed a three-dimensional finite element model of wheel–rail contact incorporating vertical cracks, revealing the competitive relationship between wear and fatigue crack propagation under rolling–sliding conditions. Regarding crack propagation and life prediction, Zhang *et al.* [126] analyzed the effects of wheel–rail dynamic characteristics, complex operating conditions, and surface defects on RCF crack initiation and proposed a corresponding prediction framework. Arana *et al.* [127] developed an RCF prediction approach that integrates crack initiation, crack propagation, and nonlinear multibody dynamics, enabling the prediction of RCF behavior across different track sections.

The literature indicates that shakedown-based stability diagrams and derived indices provide practical screening tools for surface-initiated RCF risk, while dissipated-energy damage functions and coupled wear-RCF models offer a route for joint assessment of wear and fatigue evolution.

Predictive robustness depends on representation of near-surface state change, friction variability, and thermal history and therefore requires validation against rig and field observations under representative operating spectra. The representative modeling approaches for wheel–rail wear and RCF assessment, together with their inputs, outputs, and applicability boundaries, are compared in Table III.

IV. CONDITION MONITORING AND MAINTENANCE INTERVENTIONS

As railway systems move toward higher speed, heavier axle load, and greater asset utilization, wheel damage prediction, maintenance planning, and performance restoration have become central to both running safety and whole life cost control. In parallel with network expansion, maintenance practice is increasingly shifting from fixed time or mileage-based scheduling to CBM. The effectiveness of such a transition depends on the integration of three interrelated functions: accurate condition monitoring and defect diagnosis, intervention planning that balances safety margin against material removal, and restoration or strengthening technologies that recover surface integrity and suppress recurrent damage.

This section considers wheel maintenance as a closed-loop process comprising condition monitoring and defect detection, decision-making and intervention planning, and

Table IV. Comparison of three diagnostic and monitoring paradigms for wheel/wheelset damage

Comparison dimension	Static inspection technologies	Dynamic monitoring technologies	Heterogeneous sensor data fusion technologies
Typical sensing means	Manual inspection, gauges, laser profile measurement, dedicated NDT devices, EMAT, etc.	Wayside vision, thermography, acoustic arrays, on-board/wayside vibration, laser ultrasonics, etc.	Multimodal combinations such as vibration + acoustics, vibration + acoustic emission, vibration + thermography, vision + laser, and ultrasound + vibration
Data acquisition mode	Intermittent, offline, and pointwise inspection	Continuous or periodic online acquisition covering the operating process	Synchronous or quasi-synchronous multisource acquisition, or late fusion of outputs from independent models
Main strengths	Stable inspection conditions, high signal-to-noise ratio, high accuracy, and good repeatability; suitable for quantitative defect and geometry assessment	No need for service interruption; enables automation, frequent monitoring, and early warning; well aligned with condition-based maintenance	Exploits complementarity among modalities, improves robustness, reduces false alarms, and improves generalization under complex conditions
Main limitations	Dependent on depot windows; relatively high labor and time cost; cannot cover the full-service process; early abnormalities may develop between inspections	Single sensors are vulnerable to environmental and operational disturbances, with noticeable feature drift and risks of missed or false alarms	Higher system complexity, with increased requirements for synchronization, data quality, fusion models, and computational resources
Environmental sensitivity	Relatively low because the inspection environment is usually controllable	Relatively high; vision is affected by glare, contamination, and illumination variation, acoustics by rain/snow, aerodynamic noise, and wheel–rail noise, and vibration by track excitation and mounting paths	Reduces the risk of single-channel failure through multimodal redundancy and complementarity; the most promising route for harsh environments
Real-time capability	Low	High	Medium to high, depending on the fusion level and computational architecture
Diagnostic characteristic	"High visibility and high decision"	"Early detection and wide coverage"	"Stable decision-making, disturbance resistance, and integrated assessment"
Implementation challenges	Inspection efficiency, labor dependence, disassembly requirements, and depot throughput constraints	High-speed acquisition, field noise, sensor deployment, and shortage of labeled data	Multisource asynchrony, inconsistent sampling rates, missing data, cross-modal feature alignment, and model interpretability
Suitable scenarios	Depot precision inspection, verification, wheelset withdrawal decisions, and post-maintenance acceptance	Wayside online screening, on-board continuous monitoring, and abnormality warning	Robust diagnosis in high-speed, noisy, harsh weather, and high-reliability applications
Relationship with CBM	Provides high-confidence condition references and maintenance threshold support	Provides condition tracking and early warning between depot inspections	Provides more reliable health indicators and severity assessment, making it more suitable for CBM triggering
Evaluation	A high-accuracy benchmark inspection approach, but unable to provide full-process perception	The most important engineering route for online monitoring, but limited by the robustness of single modalities	A key future direction for intelligent wheel/wheelset PHM, especially for reliable diagnosis under complex environments

reprofiling, repair, and surface reinforcement. Emphasis is placed on the translation of monitoring indicators and prediction outputs into intervention thresholds and on the feedback of intervention outcomes into subsequent assessment and trigger logic. The objective is to clarify technically defensible routes for wheelset CBM, covering depot-based and in-service monitoring, cost-effective turning and reprofiling strategies, and restoration technologies including laser cladding and surface strengthening.

A. CONDITION MONITORING AND DEFECT DETECTION

Timely and reliable detection of wheel tread defects is fundamental to the control of vibration excitation, ride quality deterioration, and in-service safety margin. In engineering practice, wheel condition assessment relies on two complementary pathways, namely depot-based inspection, which offers higher measurement fidelity under controlled conditions, and in-service monitoring, which supports earlier defect detection and interim risk control through wayside and on-board systems. More recently, data-driven diagnosis has become an increasingly important decision support tool, improving defect recognition, localization, and severity classification through large-scale inspection and monitoring datasets, while facilitating more consistent condition indicators and maintenance trigger criteria across fleets and operating environments [128].

1). DEPOT-BASED INSPECTION. Depot-based inspection is performed when vehicles are parked and, in some cases, may require wheelset disassembly. Such procedures can be labor-intensive and time-consuming and may constrain depot throughput and availability. Traditional manual inspection often relies on operator judgment using hammering, auditory cues, and basic gauges. Although widely used because of low equipment cost, manual inspection is limited by measurement resolution and repeatability and is prone to missed detection and false calls for certain defect types.

Development of optoelectronic measurement and sensor technology has enabled more instrumented depot inspection. Contact and non-contact systems using lasers and dedicated sensors can scan wheel profiles and evaluate tread geometry from measured data, reducing operator dependence and improving repeatability. Early examples include rapid tread wear and geometric deviation measurement systems developed in the United States and wheelset dimensional inspection devices developed in Japan for in-service wheelsets. In China, substantial progress has been reported for detection of tread surface and near-surface damage using electromagnetic ultrasonic techniques based on controlled excitation and reception mechanisms [129,130]. Given the maturity and broad coverage of depot-based inspection in the literature and standards, detailed discussion is not expanded further in this review, and emphasis is placed on in-service detection and intelligent diagnosis in the following subsections.

2). WAYSIDE AND ON-BOARD MONITORING. Wayside and on-board monitoring enables wheel condition assessment without stopping the vehicle, supporting rapid inspection with a high level of automation. Such dynamic approaches can provide earlier defect detection than depot-only inspection and can reduce the risk of defect growth between maintenance intervals (Fig. 9). Current practice is dominated by three technical routes: vision-based inspection, ultrasonic inspection (including electromagnetic acoustic transducer (EMAT) and laser-ultrasonic variants), and vibration-based monitoring. Increasingly, current sensing approaches are combined with data-driven diagnosis to improve defect recognition, localization, and severity assessment in operational environments.

(1) Vision- and thermography-based inspection techniques

Visual image-based inspection of railway wheel treads is a non-contact online/offline detection approach that integrates machine vision, digital image processing, and artificial intelligence, with current developments being primarily driven by deep learning. At an early stage, Japan, the United States, and Germany each developed automatic wheel inspection systems based on image processing and sensing

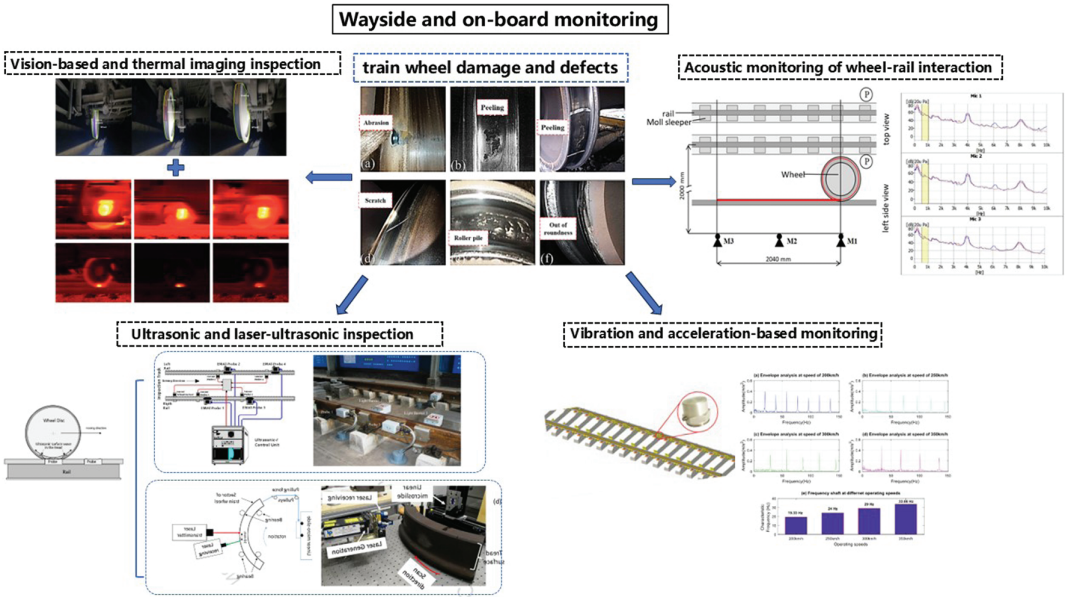

Fig. 9. Wheel wayside and on-board monitoring [135]–[146].

technologies, enabling tread parameter measurement and wear assessment under different operating speeds [131,132]. Zhao *et al.* [133] developed a system for wheel tread defect recognition and detection and investigated image region extraction techniques for the inspection process. Wu Kaihua *et al.* [134] employed laser scanning to acquire wheel tread wear images, from which the wear condition was determined through subsequent analysis and processing. During the machine learning stage, Deilamsalehy *et al.* [135,136] achieved high-accuracy wheel defect detection under thermographic imaging conditions by combining histogram of oriented gradients (HOG) features with a support vector machine (SVM) classifier, with a recognition rate of 98%. In recent years, deep learning methods have become a major research focus. Shaikh *et al.* [137] constructed the FaultSeg dataset to support the training of deep learning models for wheel damage detection. Xing *et al.* [138] developed a model for railway wheel surface defect detection that enables the classification and identification of four types of wheel tread defects. Trilla *et al.* [139] proposed a deep learning-driven method for the automatic detection and classification of wheel tread defects, in which a convolutional neural network (CNN) was used to integrate defect recognition, size prediction, and localization. Emoto *et al.* [140] further improved inspection performance by combining laser sensing and vision-based techniques with artificial intelligence models.

(2) Acoustic detection techniques based on wheel–rail interaction

Acoustic detection identifies damage by acquiring wheel–rail contact noise or vibration signals. Germany and the United States have developed online inspection devices based on ultrasonic and acoustic technologies. Komorski *et al.* [141,142] collected wheel–rail noise signals using a wayside multi-microphone array and identified wheel damage through joint time–frequency analysis (JTFA). They further combined Fourier transform and Hilbert transform for vibro-acoustic diagnosis and proposed a monitoring method for wheel tread flats, thereby enabling non-contact dynamic inspection.

(3) Ultrasonic and laser-ultrasonic inspection techniques

Ultrasonic inspection techniques can be used to identify internal and near-surface wheel defects. Salzburger *et al.* [143] proposed the AUROPA III system based on EMATs, which enables non-contact inspection at speeds of up to 15 km/h and can rapidly complete screening of an entire train. Montinaro *et al.* [144] proposed an unconventional non-contact laser-ultrasonic approach for railway wheel inspection. This method uses a laser interferometer to receive ultrasonic waves in a non-contact manner, and the receiving system allows flexible selection of the distance between the inspection surface and the interferometer, thereby overcoming spatial accessibility constraints. Cavuto *et al.* [145] further advanced laser-ultrasonic inspection technology by achieving fully non-contact inspection through laser excitation and interferometric measurement. By additionally incorporating a finite element model to optimize the inspection procedure, the method offers high inspection efficiency, strong flexibility, and non-destructive testing capability.

(4) **Wheel damage detection methods based on vibration acceleration**

Vibration acceleration-based detection methods identify wheel damage by measuring impact signals generated during wheel–rail contact. These methods are characterized by simple instrumentation and strong adaptability and have already been applied in countries such as Russia and Japan. Wang *et al.* [146] developed a vehicle-track coupled dynamic model with 73 degrees of freedom and, by combining time–frequency analysis and wavelet transform, extracted features from axle-box vibration signals to achieve accurate identification of wheel tread flats in high-speed trains.

3). MULTIMODAL SENSOR FUSION FOR ROBUST WHEEL CONDITION ASSESSMENT. Although vision-based, ultrasonic, acoustic, and vibration-based approaches are often discussed separately, multimodal sensor fusion is playing an important role in practical wheel condition monitoring. In complex railway environments, the performance of a single sensing modality may deteriorate substantially owing to variations in illumination, interference from rain and snow, aerodynamic noise, surface contaminants, installation constraints, and differences in track excitation. To address the limited robustness of single modality sensing under such demanding operating conditions, increasing research attention has been directed toward heterogeneous sensor fusion techniques for accurate fault identification in railway vehicles [147].

Existing studies have implemented fusion at three levels, namely data level, feature level, and decision level. At the data level, Deng *et al.* [148] transformed multisource signals into a unified image representation using the symmetric dot pattern method, thereby achieving raw data fusion. Combined with deep neural networks for fused feature extraction and improvement, the proposed approach demonstrated superior accuracy and noise robustness compared with both single source and conventional multisource models on public and noise-augmented datasets. Wang *et al.* [149] directly fused vibration and acoustic signals by combining a gray wolf optimizer with a SVM for rapid fault identification, further confirming the effectiveness of heterogeneous acoustic and vibration inputs in improving both detection efficiency and diagnostic accuracy.

At the feature level, Makrouf *et al.* [150] proposed a transfer learning-based framework for the fusion of vibration and acoustic features. In that method, continuous wavelet transform was first used to generate multi-sensor time–frequency representations, after which the fused wavelet coefficients were employed to fine tune a pretrained CNN. The resulting method achieved better diagnostic performance than single modality approaches under variable speed and compound fault conditions. Deng *et al.* [151] further developed an improved RSMamba network based on multidomain image fusion, in which time domain, frequency domain, and time–frequency domain features were encoded, while attention mechanisms were introduced to strengthen the identification of critical features. Such studies indicate that feature-level fusion can make fuller use of the complementary information provided by different sensing modalities and feature domains and has become one of the most representative routes in heterogeneous sensor fusion-based fault diagnosis.

At the decision level, Mey *et al.* [152] adopted a stepwise fusion strategy to integrate the diagnostic outputs of vibration and acoustic emission sensors, thereby combining low-frequency vibration information with high-frequency acoustic emission information to improve the classification accuracy of incipient damage. Compared with data-level and feature-level fusion, decision-level fusion does not require strict synchronization of raw data and offers better fault tolerance when a single sensing channel fails or its signal quality deteriorates. Such characteristics make it more suitable for online deployment in complex engineering environments.

Overall, heterogeneous sensor fusion can be implemented at the data, feature, and decision levels, corresponding respectively to joint representation of raw measurements, complementary improvement of multimodal features, and integration of independent diagnostic outputs or health indicators. Compared with single modality monitoring, multimodal fusion offers greater diagnostic robustness, lower false alarm rates, and more reliable assessment of damage severity for CBM. More importantly, static inspection, dynamic monitoring, and heterogeneous sensor fusion can be viewed as complementary components of an integrated wheel condition assessment framework. Static inspection provides high accuracy for condition confirmation and maintenance verification, dynamic monitoring supports early warning and continuous in-service tracking, and heterogeneous sensor fusion improves diagnostic reliability under complex environments and variable operating conditions. The main wheel condition monitoring and defect detection methods are summarized and compared in Table IV.

4). DATA AUGMENTATION AND SMALL-SAMPLE LEARNING FOR RARE ABNORMAL STATES. To address data scarcity in rare anomalous states, existing studies have focused on two routes for improving the generalization capability and robustness of mechanical fault diagnosis models, namely data augmentation and few shot learning.

Wright *et al.* [153] noted that conventional deep learning methods often depend on signal sampling over specific cycles or fixed time intervals, making the resulting models sensitive to sampling strategies and previously unseen operating conditions. To mitigate this limitation, they used a sliding window technique to augment phase current signals, thereby reducing the bias associated with insufficient training sample coverage and improving both classification accuracy and cross-condition generalization. In rolling bearing fault diagnosis, where model construction is often complicated and adaptability to different input forms is limited, related efforts have also increasingly explored more flexible strategies for improving model transferability and robustness. Wang *et al.* [154] proposed a general diagnostic framework based on AlexNet. In their method, raw vibration signals were transformed into fixed-size time–frequency images, and multiple time–frequency analysis techniques were employed to generate standardized inputs, thereby reducing the difficulty of model design and providing a feasible pathway for unified feature representation under few-shot conditions. Furthermore, to address the shortage of fault samples and pronounced distribution shift in railway mechanical systems under varying operating conditions, Shi *et al.* [155] combined multibody dynamics simulation with fast weighted feature space averaging to develop a data augmentation framework integrating physical priors with feature improvement. This approach not only generates simulated fault samples that more closely approximate real-world data but can also be embedded into transfer learning workflows, thereby improving model robustness under scarce fault data and varying operating conditions. From the perspective of generative modeling, Ma *et al.* [156] proposed a sparse-constrained generative adversarial network (SC-GAN), which enables stable generation of raw vibration signals through autoencoder pretraining, sparse regularization, and a two-stage training strategy. This method effectively expands samples of rare fault states and improves diagnostic accuracy and cross-device generalization in both rolling bearing and gearbox applications. Meanwhile, from the perspective of few-shot learning, Che *et al.* [157] proposed an ensemble meta-learning (EML) model, in which high-dimensional vibration signals were converted into grayscale images, meta-learning tasks were constructed, and multiple meta-learning sub-models were integrated, enabling rapid adaptation and accurate identification under few-sample and varying-condition scenarios.

Overall, above-mentioned studies indicate that data augmentation can improve the recognition of rare faults by enriching the sample distribution, whereas few shot learning and meta-learning can improve transferability and adaptability across operating conditions and diagnostic tasks when labeled data are limited. These approaches are emerging as important technical routes for addressing anomalous sample scarcity in intelligent fault diagnosis.

5). ADVANCED WEAK-FEATURE EXTRACTION UNDER HARSH OPERATIONAL ENVIRONMENTS. Under high-speed and heavy-haul operating conditions, the vibration response of wheels and wheelset systems is impacted by multiple coupled factors, including wheel–rail excitation, track irregularities, speed variation, and environmental noise, with the result that weak fault signatures are readily obscured. Conventional methods, such as Fourier transform and wavelet analysis, are effective for describing frequency domain and time–frequency characteristics but remain limited in extracting incipient damage features under strongly nonlinear, non-stationary, and low signal-to-noise ratio conditions. Advanced signal processing and intelligent identification methods have therefore attracted increasing attention as means of improving the accuracy and robustness of wheel and wheelset damage diagnosis.

Wang *et al.* [158] proposed a dynamic wheel polygonization detection method based on the iterative corrected discrete Fourier transform, which can reduce the influence of speed variation and track irregularities on detection results. To address the non-stationary characteristics of wheel vibration responses, Chen *et al.* [159] achieved quantitative detection of wheel polygonal wear under variable-speed conditions using an adaptive chirp mode decomposition method. For the recognition of tread damage images, He *et al.* [160] designed a hybrid convolutional encoding architecture for typical wheel defects, including wear, spalling, flats, and cracks, in order to enlarge the network receptive field while preserving detailed features. In addition, a cross-attention module was incorporated to suppress noise and redundant information, thereby improving the recognition accuracy of tread defects. Liu *et al.* [161] employed a field-validated three-dimensional vehicle-track coupled dynamic model and, in combination with the VMD-ES method, extracted weak

Table V. Typical wheel damage modes-observable features-detection methods-intervention measures

Damage mode	Typical causes/operating conditions	Observable signals/features	Common detection methods	Main intervention measures
Tread wear/profile evolution	Curve negotiation, adhesion variation, braking, etc.	Tread profile, equivalent conicity, wheel diameter difference	Profile measurement/online geometric inspection	Reprofiling; profile design and adaptation to operating conditions
RCF (surface/subsurface)	High contact stress, creepage, and load spectrum	Crack-related features, fatigue risk indicators	Ultrasonic testing/eddy current testing/image-based inspection	Contact condition control; reprofiling; repair and strengthening
Polygonization/out-of-roundness	Resonance excitation, braking-induced heat, coupled wheel–rail excitation	Order spectrum, axle-box vibration, roundness indicators	Dynamic monitoring (vibration/imaging)	Secondary reprofiling; strategy optimization and constraint control
White etching layer/thermal cracking	Prolonged downhill braking, thermal shock	Surface microstructural changes, thermal cracks	Visual inspection/metallographic analysis/non-destructive testing	Process and material improvement; repair and strengthening

Table VI. Applicability of wheel degradation, monitoring, and maintenance strategies across different railway systems

Railway system	Dominant degradation features	Monitoring priority	Maintenance focus	Transferability note
High-speed	Polygonal wear, out-of-roundness, stability-sensitive profile evolution	Dynamic online monitoring, weak-feature detection	Early reprofiling, stability-oriented thresholds	Sensitive to conicity and dynamic excitation
Heavy-haul	Severe wear, material loss, wear–RCF interaction	Life/depth/severity tracking	Cost-efficient life extension, robust reprofiling cycles	Strong dependence on axle load and contact stress
Urban rail	Flange wear, curve-related damage, noise issues	Frequent inspection, geometry/noise indicators	Rapid intervention, curve-wear control	Thresholds influenced by braking frequency and curve radius

features of wheel flat defects under different speeds and track irregularity conditions. The results showed that this method can extract the impact characteristics of wheel flats and achieve quantitative identification of small-sized flat defects, while still maintaining good recognition capability under the coexistence of flats and eccentricity. To address the problem that fault-related components in axle-box bearing signals are easily disturbed by track excitation and random noise, Jin *et al.* [162] proposed a fault diagnosis method based on parameter-optimized variational mode decomposition and an improved deep belief network, which improved fault feature extraction capability. Furthermore, Wang *et al.* [163] developed a reinforcement learning-based neural architecture search method that can update network structural parameters and has shown considerable potential in bearing fault diagnosis.

In summary, signal processing methods for wheel and wheelset damage diagnosis are evolving from traditional single-frequency domain analysis toward adaptive decomposition, weak impact improvement, deep feature learning, and intelligent structural optimization. Existing studies have shown that these methods offer clear advantages in suppressing complex wheel–rail background interference, improving weak fault signatures, and accommodating variable speed and non-stationary operating conditions, thereby providing more effective technical support for the early identification of train faults. Nevertheless, current research remains focused on specific defect types or laboratory-scale conditions. Future work can therefore place greater emphasis on systematic investigation under complex in-service line environments, multi-defect coupled scenarios, and cross-condition generalization. Condition monitoring can support maintenance decision-making only when measured signals are converted into interpretable condition indicators and linked to actionable thresholds. In practical application, the decision chain can include signal acquisition, feature extraction, defect and severity inference, threshold comparison, and intervention selection. Different indicators may support different maintenance actions, and the relationships among typical damage modes, observable features, detection methods, and intervention measures are summarized in Table V. Different indicators may support different maintenance actions. Profile deviation and polygonal wear metrics are closely associated with turning or reprofiling triggers, whereas crack-sensitive indicators may necessitate intensified inspection, repair, or wheel withdrawal. The value of monitoring therefore lies not only in defect detection but also in providing sufficiently robust and interpretable evidence to support the timing and selection of intervention within a CBM framework.

B. MAINTENANCE STRATEGIES AND TECHNOLOGIES

Maintenance practice in modern railways is increasingly shifting toward CBM, in which monitoring outputs, predictive models, and intervention rules are coordinated to control safety risk and whole life cost. For wheelsets, effective maintenance depends on three closely connected capabilities, namely maintenance decision-making and rule design, reprofiling quality and process control, and repair or reinforcement routes for restoring surface integrity. This

section reviews recent progress in wheel maintenance, with particular emphasis on (i) CBM decision frameworks and depot planning, (ii) reprofiling strategies that balance defect removal against material loss, and (iii) repair and reinforcement technologies for restoring surface integrity and delaying recurrent damage.

1). MAINTENANCE DECISION-MAKING AND CONDITION-BASED STRATEGIES. As railways transition from experience-based maintenance to lean CBM, maintenance decision-making is shifting from a single safety constraint toward the coordinated optimization of safety, cost, and efficiency. Optimization of maintenance strategies with the objective of minimizing life cycle cost has gradually become an important research direction in wheel–rail operation and maintenance decision-making, requiring a balance between economic efficiency and reliability under safety constraints. In terms of maintenance strategy optimization models, Liu *et al.* [164] proposed an interval-based maintenance strategy formulation method for multi-component systems with latent failures, in which the inspection intervals of individual components are determined by minimizing the long-term operating cost rate. Vafaei *et al.* [165] proposed a fuzzy early-warning method based on CBM, thereby improving diagnostic strategies within CBM frameworks. Rahimikelarijani *et al.* [166] developed a railway track maintenance decision model that integrates competing failure modes and impact-driven degradation processes and further employed Monte Carlo simulation to determine the optimal inspection intervals and intervention levels under CBM. Erguido *et al.* [167] proposed a reliability-based multi-objective maintenance model and used simulation optimization together with the NSGA-II algorithm to solve for the optimal maintenance strategy. Jiang *et al.* [168] developed a dynamic maintenance strategy based on condition monitoring information, aiming to minimize maintenance cost per unit time, and combined wheel diameter and flange thickness wear laws with a policy-iteration algorithm to determine the optimal reprofiling strategy. Sancho *et al.* [169] proposed a condition information-based optimization method for rail maintenance decision-making, in which maintenance strategies were formulated according to indicators such as rail width, rail height, accumulated million gross tonnes (MGT), and damage state, thereby reducing rail grinding costs. Zhao [170] addressed the problems of heavy maintenance workload and insufficient efficiency in electric multiple unit depots by using an optimization model for first-level maintenance scheduling based on flexible operation sequencing. With the objective of minimizing the completion time of all trainsets, the model comprehensively considered constraints such as the number of operation lines, line capacity, and operation plans and was solved using an improved GA. A case study of the Taiyuan EMU depot showed that, compared with fixed operation sequencing and a single-track-position mode, flexible operation sequencing and a double-track-position maintenance mode can improve maintenance efficiency and line utilization while shortening operation time. Wang *et al.* [171] pointed out that the wheel reprofiling interval is an important basis for determining vehicle maintenance cycles, and that coordinating the maintenance cycles of other components around the wheel reprofiling interval can reduce excessive maintenance.

Current studies present that CBM effectiveness depends on consistent linkage between condition indicators, prediction outputs, and decision rules, together with depot planning models that respect operational constraints. The key risk is that CBM triggers derived from incomplete indicators or unvalidated prediction models can shift maintenance burden without reducing system risk, leading to inefficient reprofiling schedules or unexpected wheel removals. Wheelset CBM can therefore be designed around the reprofiling cycle as an organizing constraint, with decision logic calibrated against route-specific degradation spectra and validated using measurable outcomes such as life extension, defect recurrence rate, and depot throughput.

2). INTELLIGENT DECISION-MAKING FOR MAINTENANCE. To reduce the impact of prediction drift and model overconfidence on CBM triggering, recent studies have moved beyond fixed threshold strategies toward adaptive and self-updating decision frameworks. Representative approaches include risk-informed decision support, adaptive threshold setting, online model updating, incremental learning, and dynamic optimization based on RUL feedback. Consilvio *et al.* [172] developed a risk-based decision support system in which degradation prediction is linked to maintenance intervention once a predefined risk threshold is reached, thereby reducing both unexpected failures and redundant maintenance. Lin *et al.* [173] proposed an intelligent maintenance decision method that combines multi-dimensional degradation assessment with a stochastic degradation model accounting for flange wear, polygonal wear, and wheel–rail impact and introduced an adaptive preventive-maintenance threshold mechanism. To address operating-condition drift, García *et al.* [174] incorporated online incremental classification and interpretability modules for adaptive threshold adjustment and model updating, while Martins *et al.* [175] combined statistical models, clustering, hidden Markov models, and supervised learning with a "confidence sphere" mechanism to enable self-updating prediction and dynamic threshold adaptation. For dynamic multi-objective maintenance planning, Chen *et al.* [176] employed multi-agent reinforcement learning and used RUL as feedback to continuously adjust maintenance strategy. Zhang *et al.* [177] further proposed a wheel maintenance strategy integrating periodic inspection and preventive maintenance, in which inspection intervals and reprofiling actions are optimized by minimizing maintenance cost rate under flange-thickness-related risk constraints. Although not all of these studies were developed specifically for railway wheels, they still offer useful implications for wheel CBM. In particular, they suggest that a robust maintenance framework can integrate prediction outputs with uncertainty and risk evaluation, online model updating, and adaptive intervention thresholds, rather than relying solely on fixed decision rules.

Overall, these studies indicate that mitigating drift and overconfidence in wheel CBM depends not only on improved prediction models but also on adaptive decision logic supported by uncertainty quantification, risk assessment, online updating, and threshold recalibration.

3). WHEEL REPROFILING STRATEGIES. Profile degradation during wheel–rail service can lead to stress concentration in the contact zone, deterioration in vehicle dynamic behavior, and accelerated wear and RCF. These effects impose significant constraints on the running stability of heavy-haul and urban rail vehicles and on the service life of the track system. Wheel reprofiling is therefore an essential engineering intervention for controlling wheel–rail profile

matching, slowing damage evolution, and reducing operation and maintenance costs.

With respect to wheel reprofiling, Shao *et al.* [178] reviewed the characterization methods, measurement approaches, and control standards for wheel polygonal wear and, based on operational data and tracking test results, summarized the basic characteristics and evolution patterns of polygonal wear in high-speed EMU wheels. On this basis, they proposed reprofiling control strategies for suppressing the development of wheel polygonization in high-speed EMUs. Yang *et al.* [179] conducted a comparative analysis of the evolution of wheel out-of-round wear after machining on different lathes and found that a wheel lathe with higher wheelset fixing stiffness can effectively suppress the development of higher-order out-of-round wear after reprofiling. Ren *et al.* [180] showed that when the arc length at the contact point between the wheel and the lathe driving wheel approaches an integer multiple of the wavelength of wheel polygonization, driven-wheel-positioning reprofiling may generate a pronounced form-copying effect; they further demonstrated that adjusting the spacing between the driving wheels can improve the quality of

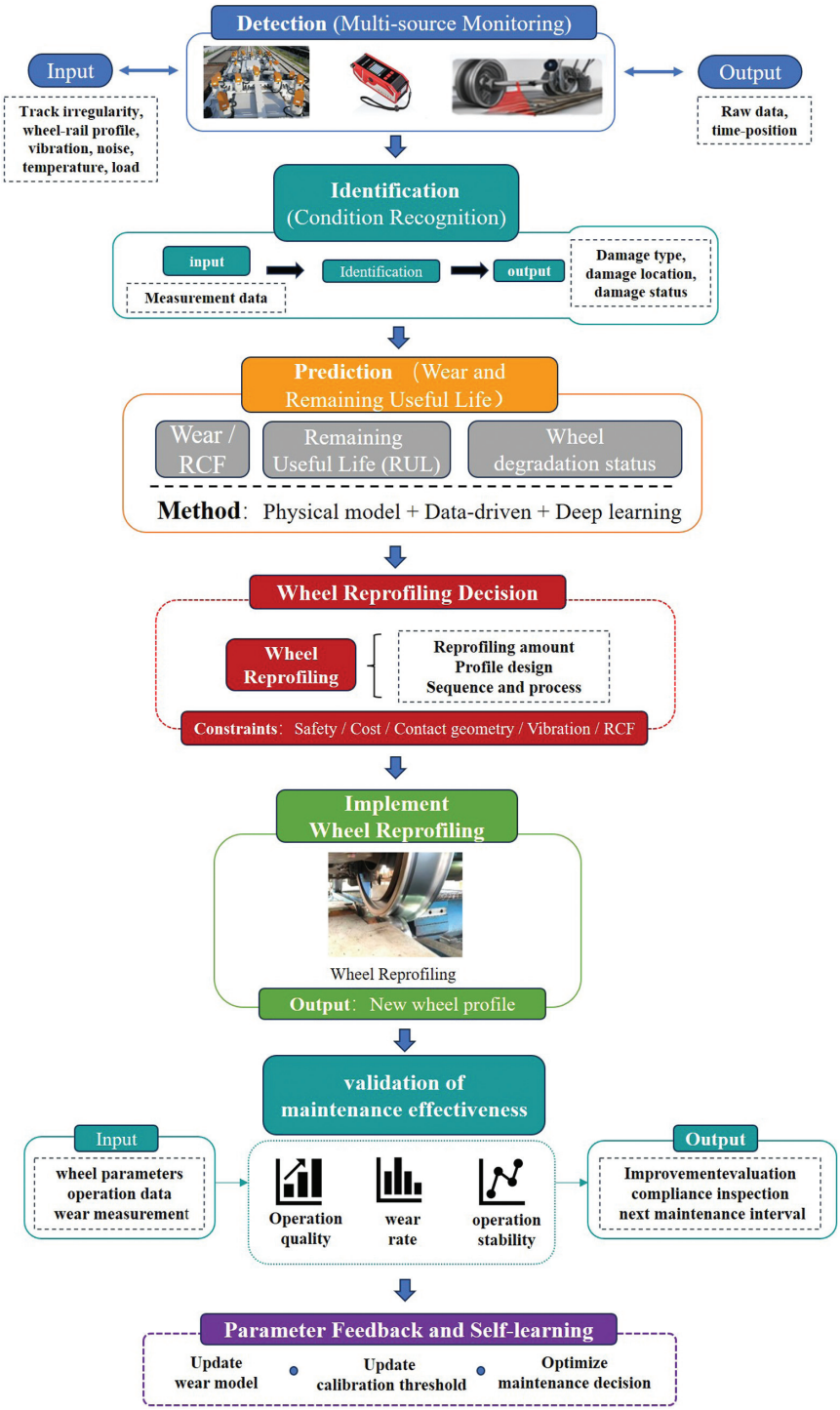

Fig 10. A closed-loop workflow for wheel reprofiling strategy formulation.

polygon reprofiling. Huang *et al.* [181] proposed an optimized reprofiling strategy for controlling the wheel diameter difference of the whole vehicle based on statistical data for wheel diameter and flange wear, which can reduce the amount of material removed during locomotive reprofiling. Liu [182] presented a flange-thinning model based on the standard thin-flange tread profile and, in combination with actual wear evolution, determined an optimal tread reprofiling scheme. By incorporating the model into an economical maintenance framework and considering factors such as the initial turning amount and wheel diameter difference, the study optimized flange thickness, material removal, and reprofiling sequence, thereby enabling customized and refined wheel reprofiling design. Cui *et al.* [183], focusing on polygonal wear associated with underfloor wheel reprofiling, proposed that secondary reprofiling can effectively eliminate higher-order polygonization. Their results further indicated that the eccentricity magnitude and phase angle of the friction roller are key factors inducing fourth-order polygonization, that the severity of this phenomenon depends on the level of eccentricity, and that roller spacing has a significant influence on reprofiling quality.

Overall, significant progress has been made in wheel polygonization control, reprofiling equipment development, and reprofiling parameter matching. Nevertheless, current studies remain centered on the optimization of wheel maintenance as an isolated component, with limited consideration of the coordinated regulation between rail grinding and wheel reprofiling under coupled wheel–rail profile matching conditions. As a result, full life cycle parameter optimization for coordinated wheel–rail maintenance has not yet been realized. Further research is therefore needed to demonstrate a closed-loop framework for wheel reprofiling strategy formulation and integrated wheel–rail maintenance, as shown in Fig. 10.

C. APPLICABILITY ACROSS DIFFERENT RAILWAY SYSTEMS

The applicability of the reviewed studies across different railway systems can be interpreted with caution, because high-speed, heavy-haul, and urban rail operations are characterized by different loading spectra, contact conditions, and maintenance constraints. In high-speed rail, operational safety and ride quality are sensitive to wheel–rail matching, equivalent conicity, out-of-roundness, and polygonal wear, such that even minor profile deviations can amplify dynamic excitation and noise. In this context, profile optimization, dynamic stability control, and early detection of weak fault signatures are of particular importance. By contrast, in heavy-haul systems, high axle loads and severe contact stresses make tread and flange wear, material loss, and the interaction between wear and RCF more dominant. Under such conditions, material selection, hardness distribution, heat treatment, surface strengthening, and cost-effective reprofiling intervals become more critical than in lighter duty applications. In urban rail and metro systems, frequent traction and braking cycles, tight curves, and limited maintenance windows place greater emphasis on flange wear, curve-related damage, noise and vibration control, and rapid inspection and intervention cycles. These differences indicate that no single monitoring, prediction, or maintenance strategy can be regarded as universally optimal. Findings obtained in one railway system can therefore not be transferred directly to another without adjustment for axle load, speed range, traction and braking duty, curve distribution, track quality, and maintenance organization. In particular, for CBM implementation, monitoring indicators, maintenance thresholds, and intervention timing can be calibrated against system-specific degradation modes and operational objectives. The applicability of wheel degradation, monitoring, and maintenance strategies across different railway systems is summarized in Table VI.

V. CONCLUSIONS AND FUTURE OUTLOOK

(1) During the design and manufacturing stage, the material system, tread geometry, and manufacturing route jointly determine the baseline wear resistance and damage tolerance of the wheel, while environment adaptive design defines the lower bound of performance under extreme service conditions. During the operational service stage, wheel–rail matching and operating conditions govern damage evolution, and both geometric evolution and risk accumulation must be considered in wear and RCF assessment. During the diagnosis and maintenance stage, static and dynamic inspection methods are complementary, whereas reprofiling and repair or strengthening measures must be coordinated under the combined constraints of geometry, vehicle dynamics, and economic efficiency. A full life cycle closed-loop framework integrating the three stages of design and manufacturing, operational service, and diagnosis and maintenance therefore represents the fundamental route to improving wheel service performance while balancing safety and cost. At present, technologies at each stage are evolving from isolated development toward coordinated optimization. Material design is shifting from a single property focus to the multi-objective coordination of strength, toughness, wear resistance, and fatigue resistance. Operation and maintenance are moving from corrective and schedule-based approaches toward predictive and CBM. Inspection and diagnosis are advancing from static single parameter detection to dynamic intelligent diagnosis based on multisource information fusion. Nevertheless, from the perspective of engineering implementation, the chain of prediction, decision, intervention, verification, and feedback has not yet been investigated. Data silos, model mismatch, and threshold inconsistency across stages remain the principal barriers to systematic improvement in service performance.

(2) The indicator and threshold system also remains insufficiently unified. During the design and manufacturing stage, the principal indicators are material strength, hardness, and microstructural uniformity. During the operational service stage, attention shifts to equivalent conicity, wear rate, and fatigue index. During the diagnosis and maintenance stage, decision-making relies more directly on indicators such as wheel diameter difference, crack depth, and vibration features. The absence of explicit mapping relationships among such stage-specific indicators makes it difficult to apply a closed-loop verification framework linking damage modes, observable signals, and intervention thresholds and may consequently lead to the coexistence of over

reprofiling and delayed risk response. In addition, the generalizability of predictive models and the quantification of uncertainty remain inadequate. Physics-based models for wear and RCF are constrained by the accuracy of contact parameter identification and by computational cost, which limits their online applicability. Data-driven models, by contrast, depend heavily on high-quality historical data and are prone to distribution drift when transferred across lines or operating conditions. More importantly, most existing models still lack effective uncertainty quantification, leaving maintenance decisions without reliable confidence bounds. A further limitation lies in the lack of coordinated wheel–rail maintenance mechanisms. Current maintenance strategies continue to focus on either the wheel or the rail as an individual component, with insufficient consideration of profile matching, hardness matching, and damage coupling within the wheel–rail system. Rail grinding and wheel reprofiling are planned and executed independently, making it difficult to support joint decision-making aimed at minimizing life cycle cost at the system level. At the same time, a contradiction remains between the robustness and real-time capability of diagnostic inspection. Dynamic inspection methods, including vibration, acoustic, and vision-based techniques, can provide high-frequency online warning but often suffer from high false alarm and missed alarm rates under complex environmental conditions such as variable illumination, rain and snow, and ambient noise. Static inspection methods, such as ultrasonic testing and profile measurement, offer higher accuracy but are performed too infrequently to support real-time decision-making. An effective linkage mechanism between dynamic early warning and static verification has therefore yet to be offered.

(3) For future engineering-oriented closed-loop implementation, research can progress systematically along four interrelated layers, namely data integration, model fusion, coordinated decision-making, and verification with feedback. First, a unified service performance indicator system and data standard can be standardized. Priority can be given to developing a standardised mapping framework linking damage mode, observable signal, assessment indicator, and intervention measure, thereby opening data interfaces across the three stages of design and manufacturing, operational service, and diagnosis and maintenance, and forming a traceable full life cycle data asset. Second, hybrid physics and data-driven modeling methods can be developed. Physics-based models can provide prior constraints and physical interpretability, whereas data-driven models can compensate for unmodeled dynamics and condition drift. At the same time, probabilistic prediction frameworks can be introduced to quantify predictive uncertainty and provide explicit risk bounds for maintenance decision-making. Third, a system-level coordinated maintenance optimization model for the wheel–rail system can be developed. Such a model can move beyond the traditional single component maintenance paradigm and support joint maintenance strategies that explicitly account for wheel–rail hardness matching, profile matching, and damage coupling, with the aim of minimising life cycle cost and achieving coordinated optimization of reprofiling intervals, grinding intervals, and maintenance actions. Fourth, a closed–loop validation mechanism covering prediction, decision, intervention, verification, and feedback can be developed. Supported by a digital twin platform, post-maintenance inspection data can be fed back to optimise design parameters, calibrate predictive models, and update decision rules, thereby forming a continuously evolving closed-loop optimization capability. In parallel, for repair and improving technologies, a complete engineering validation framework can be established, covering process windows, quality control, and in-service durability verification.

ACKNOWLEDGMENTS

This work was supported by the Major Technology Research and Development Program of the Hebei Provincial Science and Technology (24292201Z), Hebei Province Yanzhao Golden Terrace Talent Attraction Program for Outstanding Talents (A2024004), Hebei Province's Full-time Recruitment of High-level Talent Research Project (2024HBQZYCXY014), and the Science and Technology Project of the Hebei Education Department (QN2023035, CXZX2026065).

CONFLICT OF INTEREST STATEMENT

The authors declare no conflicts of interest.

REFERENCES

[1] J. B. Guinée *et al.*, "Life cycle assessment: past, present, and future," *Environ. Sci. Technol.*, vol. 45, no. 1, pp. 90–96, Jan. 2011.

[2] B. Moutik *et al.*, "Life cycle assessment research trends and implications: A bibliometric analysis," *Sustainability*, vol. 15, no. 18, p. 13408, Sep. 2023.

[3] R. D. Wahab and A. Azman, "Additive manufacturing for repair and restoration in remanufacturing: An overview from object design and systems perspectives," *Processes*, vol. 7, no. 11, pp. 802–824, Nov. 2019.

[4] D. Costa, P. Quinteiro, and A. C. Dias, "A systematic review of life cycle sustainability assessment: Current state, methodological challenges, and implementation issues," *Sci. Total Environ.*, vol. 686, pp. 774–787, Oct. 2019.

[5] J. Liu, W. Wang and Q. Liu, "Matching characteristics of four wheel materials with U71Mn hot-rolled rail," *J. Southwest Jiaotong. Univ.*, vol. 50, no. 6, pp. 1130–1136, 2015. (in Chinese)

[6] S. Chen *et al.*, "Study on the influence of wheel material properties on wheel-rail wear and fatigue performance," *Tribol*, vol. 35, no. 5, 2015. (in Chinese)

[7] W. Wang *et al.*, "Effect of carbon content on rolling friction and wear performance of wheel steel," *J. China Railw. Society*, vol. 34, no. 2, pp. 32–35, 2012. (in Chinese)

[8] P. Wen *et al.*, "Influence of microstructure on properties of high-power locomotive wheel material," *Heat Treat. Met.*, vol. 37, no. 5, pp. 6–10, 2012. (in Chinese)

[9] P. Sun *et al.*, "Experimental study on friction and wear of new CL60 steel subway wheels," *Lubr. Eng.*, vol. 48, no. 6, pp. 32–37, 2023. (in Chinese)

[10] T. Pan *et al.*, "Alloy design of anti-spalling wheel steel and effect of Si on anti-spalling performance," *Iron Steel*, vol. 44, no. 8, pp. 67–71, 2009. (in Chinese)
[11] D. Zeng *et al.*, "Optimisation of strength and toughness of railway wheel steel by alloy design," *Mater. Des.*, vol. 92, pp. 998–1006, Feb. 2016.
[12] L. F. Demisie, M. G. Wedajeneh, and A. A. Ejigu, "Effect of compositions and hardness on wheel-rail contact analysis and wear behavior of wheel materials using finite element method: a case study of addis ababa light rail transit," *Discov. Mater.*, vol. 5, no. 1, p. 115, Jul. 2025.
[13] T. Jia *et al.*, "Study on mechanism and influencing factors of wheel strengthening and toughening of high-speed and heavy-load train," *Crystals*, vol. 13, no. 1, p. 81, Jan. 2023.
[14] R. Devanathan and P. Clayton, "Rolling-sliding wear behavior of three bainitic steels," *Wear*, vol. 151, no. 2, pp. 255–267, Dec. 1991.
[15] J. Kalousek, D. M. Fegredo, and E. E. Laufer, "The wear resistance and worn metallography of pearlite, bainite and tempered martensite rail steel microstructures of high hardness," *Wear*, vol. 105, no. 3, pp. 199–222, Oct. 1985.
[16] U. P. Singh *et al.*, "Microstructure and mechanical properties of as rolled high strength bainitic rail steels," *Mater. Sci. Technol.*, vol. 17, no. 1, pp. 33–38, Jan. 2001.
[17] K. M. Lee and A. A. Polycarpou, "Wear of conventional pearlitic and improved bainitic rail steels," *Wear*, vol. 259, no. 1–6, pp. 391–399, Jul. 2005.
[18] C. C. Viáfara *et al.*, "Unlubricated sliding wear of pearlitic and bainitic steels," *Wear*, vol. 259, no. 1–6, pp. 405–411, Jul. 2005.
[19] D. Zapata, J. Jaramillo, and A. Toro, "Rolling contact and adhesive wear of bainitic and pearlitic steels in low load regime," *Wear*, vol. 271, no. 1–2, pp. 393–399, May 2011.
[20] S. M. Hasan, D. Chakrabarti, and S. B. Singh, "Dry rolling/sliding wear behaviour of pearlitic rail and newly developed carbide-free bainitic rail steels," *Wear*, vol. 408–409, pp. 151–159, Aug. 2018.
[21] S. Sharma, S. Sangal, and K. Mondal, "Wear behavior of newly developed bainitic wheel steels," *J. Mater. Eng. Perform.*, vol. 24, no. 2, pp. 999–1010, Feb. 2015.
[22] Y. Chen *et al.*, "Microstructure evolution of rail steels under different dry sliding conditions: a comparison between pearlitic and bainitic microstructures," *Wear*, vol. 438–439, p. 203011, Nov. 2019.
[23] J. P. Liu *et al.*, "New insight into the dry rolling-sliding wear mechanism of carbide-free bainitic and pearlitic steel," *Wear*, vol. 432–433, p. 202943, Aug. 2019.
[24] A. B. Rezende *et al.*, "Wear behavior of bainitic and pearlitic microstructures from microalloyed railway wheel steel," *Wear*, vol. 456–457, p. 203377, Sep. 2020.
[25] M. R. Zhang and H. C. Gu, "Microstructure and properties of carbide free bainite railway wheels produced by programmed quenching," *Mater. Sci. Technol.*, vol. 23, no. 8, pp. 970–974, Aug. 2007.
[26] F. Movassagh-Alanagh and M. Mahdavi, "Improving wear and corrosion resistance of AISI 304 stainless steel by a multilayered nanocomposite Ti/TiN/TiSiN coating," *Surf. Interfaces*, vol. 18, p. 100428, Mar. 2020.
[27] X. Ding *et al.*, "Structure and cavitation erosion behavior of HVOF sprayed multi-dimensional WC–10Co4Cr coating," *Trans. Nonferr. Met. Soc. China*, vol. 28, no. 3, pp. 487–494, Mar. 2018.
[28] H. Ding *et al.*, "Microstructure and wear performance of h-BN/CaF_2/Fe-based laser cladding coating on wheel material surface," *China Surf. Eng.*, vol. 34, no. 4, pp. 139–148, 2021. (in Chinese)
[29] Z. B. Wang *et al.*, "Effect of surface nanocrystallisation on friction and wear properties in low carbon steel," *Mater. Sci. Eng. A*, vol. 352, no. 1–2, pp. 144–149, Jul. 2003.
[30] W. Wang *et al.*, "Effect of laser quenching on wear and damage of heavy-haul wheel/rail materials," Proc. Inst. Mech. Eng. Part J J. Eng. Tribol., vol. 228, no. 1, pp. 114–122, Jan. 2014.
[31] N. Zhao *et al.*, "Microstructure and kinetics study on tantalum carbide coating produced on gray cast iron in situ," *Surf. Coat. Technol.*, vol. 286, pp. 347–353, Jan. 2016.
[32] H. Bai *et al.*, "Microstructure and fracture toughness of compact TiC-Fe gradient coating fabricated on cast iron substrate by two-step In situ reaction," *JOM*, vol. 72, no. 6, pp. 2154–2163, Jun. 2020.
[33] A. Sadeghi *et al.*, "Effect of initial texture and microstructure of Mg on mechanical properties of Mg–stainless steel laminated metal composites," *Mater. Charact.*, vol. 127, pp. 171–178, May 2017.
[34] J. Y. Kang *et al.*, "Outstanding mechanical properties of high-pressure torsion processed multiscale TWIP-cored three layer steel sheet," *Scr. Mater.*, vol. 123, pp. 122–125, Oct. 2016.
[35] H. Wu *et al.*, "Fabrication and mechanical properties of TiBw/Ti-Ti(Al) laminated composites," *Mater. Des.*, vol. 89, pp. 697–702, Jan. 2016.
[36] I. Y. Shevtsov, V. L. Markine, and C. Esveld, "Optimal design of wheel profile for railway vehicles," *Wear*, vol. 258, no. 7–8, pp. 1022–1030, Mar. 2005.
[37] D. Cui *et al.*, "Optimal design of wheel profiles based on weighed wheel/rail gap," *Wear*, vol. 271, no. 1–2, pp. 218–226, May 2011.
[38] J. Santamaria *et al.*, "Design of an optimised wheel profile for rail vehicles operating on two-track gauges," *Veh. Syst. Dyn.*, vol. 51, no. 1, pp. 54–73, Jan. 2013.
[39] F. Meng *et al.*, "Optimisation of JM3 wheel profile considering equivalent conicity dispersion, "J. Southwest Jiaotong Univ., vol. 60, no. 2, pp. 346–355, 2025. (in Chinese)
[40] D. Cui *et al.*, "Multi-objective optimisation of electric multiple unit wheel profile from wheel flange wear viewpoint," *Struct. Multidiscip. Optim.*, vol. 59, no. 1, pp. 279–289, Jan. 2019.
[41] Y. Fu *et al.*, "Wheel profile optimisation of speed-up freight train based on multi-population genetic algorithm".
[42] M. Hou *et al.*, "Wheel profile optimisation for intercity EMUs based on the gaussian function correction method," *Proc. Inst. Mech. Eng. Part F J. Rail Rapid Transit.*, vol. 238, no. 7, pp. 775–785, Aug. 2024.
[43] H.-Y. Choi, D.-H. Lee, and J. Lee, "Optimisation of a railway wheel profile to minimise flange wear and surface fatigue," *Wear*, vol. 300, no. 1–2, pp. 225–233, Mar. 2013.
[44] P. A. De Paula Pacheco *et al.*, "Optimisation of heavy haul railway wheel profile based on rolling contact fatigue and wear performance," *Wear*, vol. 522, p. 204704, Jun. 2023.
[45] Y. Lu *et al.*, "Optimisation and design of a railway wheel profile based on interval uncertainty to reduce circular wear," Math. Probl. Eng., vol. 2020, pp. 1–10, Oct. 2020.
[46] B. Firlik *et al.*, "Optimisation of a tram wheel profile using a biologically inspired algorithm," *Wear*, vol. 430–431, pp. 12–24, Jul. 2019.
[47] F. Gan *et al.*, "Calculation of equivalent conicity and wheel-rail contact relationship for different treads of

railway vehicles," *J. China Railw. Society*, vol. 35, no. 9, pp. 19–24, 2013. (in Chinese)

[48] Y. Qian *et al.*, "Development and application of a calculation method for the equivalent conicity in high-speed turnout zones," *Veh. Syst. Dyn.*, vol. 60, no. 1, pp. 96–113, Jan. 2022.

[49] P. Damsongsaeng *et al.*, "Estimation of wheelset equivalent conicity using the dual extended kalman filter," *Multibody Syst. Dyn.*, vol. 60, no. 4, pp. 563–579, Apr. 2024.

[50] Z. Xu and X. Dong, "Research and verification on the nonlinear characteristics of wheel/rail equivalent conicity," in Advances in Dynamics of Vehicles on Roads and Tracks, M. Klomp, F. Bruzelius, J. Nielsen, and A. Hillemyr, Eds., in Lecture Notes in Mechanical Engineering., Cham: Springer International Publishing, 2020, pp. 678–685.

[51] R. Kulkarni *et al.*, "Investigating the effect of the equivalent conicity function's nonlinearity on the dynamic behaviour of a rail vehicle under typical service conditions," *Veh. Syst. Dyn.*, vol. 60, no. 10, pp. 3484–3503, Oct. 2022.

[52] J. Gerlici *et al.*, "Calculated estimation of railway wheels equivalent conicity influence on critical speed of railway passenger car," *MATEC Web Conf.*, vol. 157, p. 3006, 2018.

[53] R. Chen *et al.*, "Optimisation of turnout rail profiles based on equivalent conicity," *Veh. Syst. Dyn.*, vol. 60, no. 9, pp. 3071–3087, Sep. 2022.

[54] I. Persson and L.-O. Jönsson, "Gradient index profile, a novel idea for predicting equivalent conicity," in Advances in Dynamics of Vehicles on Roads and Tracks II, A. Orlova and D. Cole, Eds., in Lecture Notes in Mechanical Engineering., Cham: Springer International Publishing, 2022, pp. 513–521.

[55] Y. Tian *et al.*, "A novel quenching strategy for improved mechanical behaviour homogeneity of large-size parts via bainite kinetics acceleration: Experimental and numerical investigation," *J. Manuf. Process.*, vol. 124, pp. 843–855, Aug. 2024.

[56] Y. Zhang *et al.*, "Stress relief during annealing of railway wheel steel characterised by synchrotron X-ray microdiffraction," *IOP Conf. Ser. Mater. Sci. Eng.*, vol. 1249, no. 1, p. 12043, Jul. 2022.

[57] B. Gao *et al.*, "Design of quenching and tempering process and elucidation of the relationship between microstructure and properties of 20Mn2SiNiMo bainitic wheel steel," *Steel Res. Int.*, vol. 95, no. 9, p. 2400109, Sep. 2024.

[58] J. Liu *et al.*, "Study on wear and rolling contact damage mechanism between quenched U75V rail and wheels with different microstructures," *Wear*, vol. 512–513, p. 204544, Jan. 2023.

[59] Q. Zhang *et al.*, "Influence of laminar plasma quenching on rolling contact fatigue behaviour of high-speed railway wheel steel," *Int. J. Fatigue*, vol. 137, p. 105668, Aug. 2020.

[60] K. Wang *et al.*, "Effect of material non-uniformity and residual stress on wear and transient rolling contact behaviour in laminar plasma quenched (LPQ) rails," *Wear*, vol. 523, p. 204767, Jun. 2023.

[61] D. Li *et al.*, "Quantitative distribution characterisation and correlation study of composition, structure and hardness of rim region in railway wheel," *Materials (Basel)*, vol. 15, no. 14, p. 4762, Jul. 2022.

[62] S. N. Lingamanaik and B. K. Chen, "Thermo-mechanical modelling of residual stresses induced by martensitic phase transformation and cooling during quenching of railway wheels," *J. Mater. Process. Technol.*, vol. 211, no. 9, pp. 1547–1552, Sep. 2011.

[63] J. L. Cuperus, G. Venter, and D. C. Blaine, "Finite element analysis of the tread quenching of railway wheels," pp. 0–14.

[64] Y. Tian *et al.*, "Experiment and finite element analysis of asymmetrical hardness induced by quenching in railway wheel," *Eng. Fail. Anal.*, vol. 133, p. 105959, Mar. 2022.

[65] J. Xiong, T. Zhang, and S. Shi, "Machine learning of mechanical properties of steels," *Sci. China Technol. Sci.*, vol. 63, no. 7, pp. 1247–1255, Jul. 2020.

[66] E. K. Isakaev *et al.*, "Plasma hardening of railway wheel surface," presented at the APS Annual Gaseous Electronics Meeting Abstracts, Oct. 1998, p. OWP4.1. Accessed: Oct. 05, 2025. [Online]. Available: I

[67] A. T. Kanaev *et al.*, "Improving the wear resistance of wheel-pair rims by plasma quenching," *Steel Transl.*, vol. 42, no. 6, pp. 544–547, Jun. 2012.

[68] D. I. Yusupov *et al.*, "Plasma hardening as an effective way to increase the resource of solid-rolled wheels of freight cars," presented at the 2ND INTERNATIONAL CONFERENCE & EXPOSITION ON MECHANICAL, MATERIAL, AND MANUFACTURING TECHNOLOGY (ICE3MT 2022), Hyderabad, India, 2023, p. 20005.

[69] A. V. Bogdanov *et al.*, "Increasing microhardness and hardening depth of grade 2 wheel steel using fiber lasers," presented at the XLIII ACADEMIC SPACE CONFERENCE: dedicated to the memory of academician S.P. Korolev and other outstanding Russian scientists–Pioneers of space exploration, Moscow, Russia, 2019, p. 200004.

[70] S. I. Gubenko *et al.*, "Improving the properties of wheeled steel during thermal repair," *IOP Conf. Ser. Mater. Sci. Eng.*, vol. 971, no. 5, p. 52067, Nov. 2020.

[71] X. Cao *et al.*, "Investigation on the microstructure and damage characteristics of wheel and rail materials subject to laser dispersed quenching," *Appl. Surf. Sci.*, vol. 450, pp. 468–483, Aug. 2018.

[72] S. Fayzibaev *et al.*, "Hardening the rolling surface of the wheels bandage after mechanical treatment," *E3S Web Conf.*, vol. 458, p. 10003, 2023.

[73] S. Gubenko, "About the possibility of local laser hardening of the treed of railway wheels".

[74] L. B. Shi *et al.*, "Influence of low temperature environment on the adhesion characteristics of wheel-rail contact," *Tribol. Int.*, vol. 127, pp. 59–68, Nov. 2018.

[75] L. Zhou *et al.*, "Experimental study on the wear and damage of wheel-rail steels under alternating temperature conditions," *Wear*, vol. 477, p. 203829, Jul. 2021.

[76] O. P. Ostash *et al.*, "Low-temperature cyclic crack resistance of steels of railroad wheels," *Mater. Sci.*, vol. 44, no. 4, pp. 524–529, Jul. 2008.

[77] J. X. Li *et al.*, "Wear and damage behaviours of wheel and rail materials: Effects of friction modifier and environmental temperature," *Wear*, vol. 523, p. 204796, Jun. 2023.

[78] Z. Liang *et al.*, "Introducing nano-VC precipitates makes ultrafine bainitic steel a better combination of strength, ductility, and toughness," *Mater. Res. Lett.*, vol. 12, no. 10, pp. 756–763, Oct. 2024.

[79] K. Rong *et al.*, "Influence of ambient humidity on the adhesion and damage behavior of wheel–rail interface under hot weather condition," *Wear*, vol. 486–487, p. 204091, Dec. 2021.

[80] C. He *et al.*, "Experimental investigation of the wear and damage of CL60 wheel material in a humid hot

environment," *J. Mater. Eng. Perform.*, vol. 32, no. 8, pp. 3500–3514, Apr. 2023.
[81] C. He *et al.*, "Effects of various laser cladding materials on the tribological properties of damaged wheel treads under various temperatures and humidities," *Tribol. Int.*, vol. 202, p. 110374, Feb. 2025.
[82] J. Li *et al.*, "Study on Hardness Matching of Wheel and Rail," *China Railw. Sci.*, vol. 5, no. 1, pp. 49–59, 1984. (in Chinese).
[83] H. Ding *et al.*, "Rolling wear and damage behavior of three rail materials matched with wheels," *Tribol*, vol. 34, no. 3, pp. 233–239, 2014. (in Chinese)
[84] R. Stock, D. Eadie, and K. Oldknow, "Rail grade selection and friction management: A combined approach for optimising rail–wheel contact," *Ironmak. Steelmak.*, vol. 40, no. 2, pp. 108–114, Feb. 2013.
[85] S. Zhou *et al.*, "Friction and wear test of high-speed wheel material and U71MnG rail material," *Railw. Eng.*, vol. 57, no. 9, pp. 128–131, 2017. (in Chinese)
[86] H. Zhao *et al.*, "Effect of wheel-rail hardness matching on wear performance of heavy-Haul Bainitic wheel steel," *Surf. Technol.*, vol. 54, no. 3, pp. 118–129, 2025. (in Chinese)
[87] Y. Hu *et al.*, "Experimental study on wear properties of wheel and rail materials with different hardness values," *Wear*, vol. 477, p. 203831, Jul. 2021.
[88] W. Wang, Q. Liu, and M. Zhu, "Experimental study on hardness matching performance of wheel and rail materials," *Tribol*, vol. 33, no. 1, pp. 65–69, 2013. (in Chinese)
[89] Y. Hu *et al.*, "Investigation on wear and rolling contact fatigue of wheel-rail materials under various wheel/rail hardness ratio and creepage conditions," *Tribol. Int.*, vol. 143, p. 106091, Mar. 2020.
[90] Y. Zhang *et al.*, "Experimental study on wheel-rail hardness matching for high-speed railway," *China Railw. Sci.*, vol. 38, no. 4, pp. 1–7, 2017. (in Chinese)
[91] C. Chang *et al.*, "Experimental study on effect of wheel-rail material hardness matching on wheel polygonal wear," *China Railw. Sci.*, vol. 39, no. 2, pp. 87–93, 2018. (in Chinese)
[92] T. Ma and G. Zhu, "Study on rail/wheel matching relationship of heat-treated rails," *Phys. Exam. Test.*, vol. 17, no. 5, pp. 1–3, 1999. (in Chinese)
[93] D. Sherratt, "Prediction of wheel profile wear," *Wear*, vol. 144, no. 1–2, p. 343–351, Apr. 1991.
[94] A. Bevan *et al.*, "Development and validation of a wheel wear and rolling contact fatigue damage model," *Wear*, vol. 307, no. 1–2, pp. 100–111, Sep. 2013.
[95] Z. Wang *et al.*, "Wheel wear analysis of motor and unpowered car of a high-speed train," *Wear*, vol. 444–445, p. 203136, Mar. 2020.
[96] C. Chang, C. Wang, and Y. Jin, "Numerical analysis of wheel-rail wear based on three-dimensional dynamic finite element model," *China Railw. Sci.*, vol. 29, no. 4, pp. 89–95, 2008. (in Chinese)
[97] H. Sang *et al.*, "Study on wheel wear mechanism of high-speed train in accelerating conditions," *Wear*, vol. 516–517, p. 204597, 2023.
[98] F. Braghin *et al.*, "A mathematical model to predict railway wheel profile evolution due to wear," *Wear*, vol. 261, no. 11, pp. 1253–1264, Dec. 2006.
[99] P. Wang *et al.*, "Development of a wheel wear prediction model considering the interaction of abrasive block–wheel and wheel–rail," *Wear*, vol. 551, p. 205418, 2024.
[100] J. Niu *et al.*, "Prediction analysis of wheel wear based on semi-hertzian contact," *China Mech. Eng.*, vol. 34, no. 7, pp. 859–865, 874, 2023. (in Chinese)
[101] G. Tao *et al.*, "Effects of wheel-rail contact modelling on wheel wear simulation," *Wear*, vol. 366–367, pp. 146–156, May 2016.
[102] Y. Yang *et al.*, "Comparison of wheel/rail contact modelling in prediction of wheel tread wear under changeable friction conditions," *Veh. Syst. Dyn.*, vol. 64, no. 1, pp. 125–154, 2026.
[103] W. Zhu *et al.*, "Data-driven wheel wear modeling and reprofiling strategy optimisation for metro systems," *Transp. Res. Rec. J. Transp. Res. Board*, vol. 2476, no. 1, pp. 67–76, Jan. 2015.
[104] M. De Almeida Costa, J. P. De Azevedo Peixoto Braga, and A. Ramos Andrade, "A data-driven maintenance policy for railway wheelset based on survival analysis and markov decision process," *Qual. Reliab. Eng. Int.*, vol. 37, no. 1, pp. 176–198, Feb. 2021.
[105] Z. Chi *et al.*, "Data-driven approach to study the polygonisation of high-speed railway train wheel-sets using field data of China's HSR train," *Measurement*, vol. 149, p. 107022, Jan. 2020.
[106] A. Shebani and S. Iwnicki, "Prediction of wheel and rail wear under different contact conditions using artificial neural networks," *Wear*, vol. 406–407, pp. 173–184, Jul. 2018.
[107] Y. Deng *et al.*, "A data-driven wheel wear prediction model for rail train based on LM-OMP-NARXNN," *J. Comput. Inf. Sci. Eng.*, vol. 23, no. 2, p. 021012, Apr. 2023.
[108] A. Shangguan *et al.*, "Train wheel degradation generation and prediction based on the time series generation adversarial network," *Reliab. Eng. Syst. Saf.*, vol. 229, p. 108816, Jan. 2023.
[109] S. Liu *et al.*, "A two-step data-driven method for predicting the wear of train wheel treads using GA-BPNN and LSTM algorithms," *Int. J. Rail Transp.*, vol. 13, no. 1, pp. 85–102, Jan. 2025.
[110] Y. Ye *et al.*, "Predicting railway wheel wear by calibrating existing wear models: Principle and application," *Reliab. Eng. Syst. Saf.*, vol. 238, p. 109462, Oct. 2023.
[111] Y. Zeng *et al.*, "A new physics-based data-driven guideline for wear modelling and prediction of train wheels," *Wear*, vol. 456–457, p. 203355, Sep. 2020.
[112] R. Wang *et al.*, "Optimisation of wheelset maintenance strategies using a combination of physical and data- driven models". *The 13th World Congress on Railway Research (WCRR), The International Convention Centre in Birmingham*, 2022.
[113] A. Zhu *et al.*, "Research on prediction of metro wheel wear based on integrated data-model-driven approach," *IEEE Access*, vol. 7, pp. 178153–178166, 2019.
[114] D. Hartwich *et al.*, "A new hybrid approach to predict worn wheel profile shapes," *Veh. Syst. Dyn.*, vol. 61, no. 6, pp. 1548–1564, Jun. 2023.
[115] K. L. Johnson, "The strength of surfaces in rolling contact," *Proc. Inst. Mech. Eng. Part C Mech. Eng. Sci.*, vol. 203, no. 3, pp. 151–163, May. 1989.
[116] A. R. S. Ponter, A. D. Hearle, and K. L. Johnson, "Application of the kinematical shakedown theorem to rolling and sliding point contacts," *J. Mech. Phys. Solids*, vol. 33, no. 4, pp. 339–362, Jan. 1985.

[117] K. L. Johnson, "A graphical approach to shakedown in rolling contact," in Applied Stress Analysis, T. H. Hyde and E. Ollerton, Eds., Dordrecht: Springer Netherlands, 1990, pp. 263–274.
[118] A. F. Bower and K. L. Johnson, "Plastic flow and shakedown of the rail surface in repeated wheel-rail contact," *Wear*, vol. 144, no. 1, pp. 1–18, Apr. 1991.
[119] F. Salas Vicente and M. Pascual Guillamón, "Use of the fatigue index to study rolling contact wear," *Wear*, vol. 436–437, p. 203036, Oct. 2019.
[120] B. Dirks and R. Enblom, "Prediction model for wheel profile wear and rolling contact fatigue," *Wear*, vol. 271, no. 1, pp. 210–217, May 2011.
[121] P. J. Bolton and P. Clayton, "Rolling—sliding wear damage in rail and tyre steels," *Wear*, vol. 93, no. 2, pp. 145–165, Jan. 1984.
[122] E. Butini *et al.*, "An innovative model for the prediction of wheel - rail wear and rolling contact fatigue," *Wear*, vol. 436–437, p. 203025, Oct. 2019.
[123] Y. Dong *et al.*, "Prediction of fatigue crack initiation life on wheel tread during emergency braking of heavy-Haul train," *China Railw. Sci.*, vol. 42, no. 5, pp. 123–131, 2021. (in Chinese)
[124] A. Mazzù and G. Donzella, "A model for predicting plastic strain and surface cracks at steady-state wear and ratcheting regime," *Wear*, vol. 401–401, pp. 127–136, Apr. 2018.
[125] X. Zhou *et al.*, "Fatigue crack growth in wheel-rail rolling-sliding contact: A perspective of elastic-plastic fracture mechanics criterion," *Wear*, vol. 531–531, p. 205069, Oct. 2023.
[126] S. Zhang *et al.*, "Gaps, challenges and possible solution for prediction of wheel–rail rolling contact fatigue crack initiation," *Railw. Eng. Sci.*, vol. 31, no. 3, pp. 207–232, Sep. 2023.
[127] B. Rodríguez-Arana *et al.*, "Prediction of rolling contact fatigue behavior in rails using crack initiation and growth models along with multibody simulations," *Appl. Sci.*, vol. 11, no. 3, p. 1026, Jan. 2021.
[128] J. Zeng *et al.*, "Review of wheel flat fault detection technology for railway vehicles," *J. Traffic Transp. Eng.*, vol. 22, no. 2, pp. 1–18, 2022. (in Chinese)
[129] S. Wang, Z. Zhao, and G. Zhai, "Train wheel crack detection system based on electromagnetic ultrasound," *Instrum. Tech. Sens.*, no. 11, pp. 30–32, 2005. (in Chinese)
[130] W. Wang *et al.*, "Data-driven prediction method for wheel tread defects of head and tail cars of high-speed railway EMUs," *Urban Mass Transit. Res.*, vol. 27, no. 4, pp. 28–32, 2024. (in Chinese)
[131] X. Zhang, J. Xu, and G. Ge, "Defects recognition on X-ray images for weld inspection using SVM," in Proceedings of 2004 International Conference on Machine Learning and Cybernetics (IEEE Cat. No.04ex826), Shanghai, China: IEEE, 2004, pp. 3721–3725.
[132] R. Liang *et al.*, "Copper strip surface defects inspection based on SVM-RBF," in 2008 Fourth International Conference on Natural Computation, Jinan, Shandong, China: IEEE, 2008, pp. 41–45.
[133] Y. Zhao, "A fast image segmentation method for light section curve of wheel tread," *Application Electron. Tech.*, vol. 37, no. 3, pp. 130–132, 136, 2011. (in Chinese)
[134] K. Wu and K. Yan, "Research on photoelectric detection method for tread defects of vehicle wheelset," *Opt. Tech.*, no. 3, pp. 465–467, 2005. (in Chinese)
[135] H. Deilamsalehy *et al.*, "An automatic method for detecting sliding railway wheels and hot bearings using thermal imagery," Proc. Inst. Mech. Eng. Part F J. Rail Rapid Transit., vol. 231, no. 6, pp. 690–700, Jul. 2017.
[136] H. Deilamsalehy, T. C. Havens, and P. Lautala, "Detection of sliding wheels and hot bearings using wayside thermal cameras," in 2016 Joint Rail Conference, Columbia, South Carolina, USA: American Society of Mechanical Engineers, Apr. 2016, p. V001T02A002.
[137] M. Z. Shaikh *et al.*, "FaultSeg: A dataset for train wheel defect detection," *Sci. Data*, vol. 12, no. 1, p. 309, Feb. 2025.
[138] Z. Xing *et al.*, "Rail wheel tread defect detection using improved YOLOv3," *Measurement*, vol. 203, p. 111959, Nov. 2022.
[139] A. Trilla *et al.*, "Integrated multiple-defect detection and evaluation of rail wheel tread images using convolutional neural networks," *Int. J. Progn. Health Manag.*, vol. 12, no. 1, May 2021.
[140] T. Emoto *et al.*, "Automatic inspection of wheel surface defects using a combination of laser sensors and machine vision," *SICE J. Control Meas. Syst. Integr.*, vol. 17, no. 1, pp. 57–66, Dec. 2024.
[141] P. Komorski *et al.*, "Application of time-frequency analysis of acoustic signal to detecting flat places on the rolling surface of a tram wheel," in *Dynamical Systems in Applications, vol. 249, J. Awrejcewicz, Ed., in Springer Proceedings in Mathematics & Statistics*, vol. 249., Cham: Springer International Publishing, 2018, pp. 205–215.
[142] P. Komorski *et al.*, "Advanced acoustic signal analysis used for wheel-flat detection," *Lat. Am. J. Solids Struct.*, vol. 18, no. 1, p. e338, 2021.
[143] H. J. Salzburger *et al.*, "In-motion ultrasonic testing of the tread of high-speed railway wheels using the inspection system AUROPA III," *Insight - Non-Destr. Test. Cond. Monit.*, vol. 51, no. 7, pp. 370–372, Jul. 2009.
[144] N. Montinaro *et al.*, "Laser ultrasonics inspection for defect evaluation on train wheel," *NDT E Int.*, vol. 107, p. 102145, Oct. 2019.
[145] A. Cavuto *et al.*, "Train wheel diagnostics by laser ultrasonics," *Measurement*, vol. 80, pp. 99–107, Feb. 2016.
[146] R. Wang *et al.*, "Vibration-based detection of wheel flat on a high-speed train," in Advances in *Asset Management* and *Condition Monitoring*, vol. 166, A. Ball, L. Gelman, and B. K. N. Rao, Eds., in Smart Innovation, Systems and Technologies, vol. 166, Cham: Springer International Publishing, 2020, pp. 159–169.
[147] W. Fu *et al.*, "Recent advances in wayside railway wheel flat detection techniques: A review," *Sensors*, vol. 23, no. 8, Art. no. 3916, Apr. 2023.
[148] X. Deng *et al.*, "A multi-level fusion framework for bearing fault diagnosis using multi-source information," *Processes*, vol. 13, no. 8, Art. 2184, Aug. 2025.
[149] T. Wang *et al.*, "Fault detection of wheelset bearings through vibration-sound fusion data based on grey wolf optimiser and support vector machine," *Technologies.*, vol. 12, no. 9, Art. no. 144, Aug. 2024.
[150] I. Makrouf *et al.*, "A novel framework for multi-sensor data fusion in bearing fault diagnosis using continuous wavelet transform and transfer learning," *E-Prime - Adv. Electr. Eng. Electron. Energy*, vol. 13, p. 101025, Sep. 2025.
[151] F. Deng *et al.*, "An improved RSMamba network based on multi-domain image fusion for wheelset bearing fault diagnosis under composite conditions," *J. Comput. Des. Eng.*, vol. 12, no. 3, pp. 65–79, Mar. 2025.
[152] O. Mey *et al.*, "Condition monitoring of drive trains by data fusion of acoustic emission and vibration sensors," *Processes*, vol. 9, no. 7, Art. no. 1108, Jun. 2021.

[153] R. Wright *et al.*, "Improved fault detection using shifting window data augmentation of induction motor current signals," *Energies*, vol. 17, no. 16, Art. no. 3956, Aug. 2024.
[154] J. Wang *et al.*, "A deep learning method for bearing fault diagnosis based on time-frequency image," *IEEE Access*, vol. 7, pp. 42373–42383, 2019.
[155] D. Shi *et al.*, "Robustness improvement of machine fault diagnostic models for railway applications through data augmentation," *Mech. Syst. Signal Process.*, vol. 164, p. 108217, Feb. 2022.
[156] L. Ma *et al.*, "An interpretable data augmentation scheme for machine fault diagnosis based on a sparsity-constrained generative adversarial network," *Expert Syst. Appl.*, vol. 182, p. 115234, Nov. 2021.
[157] C. Che *et al.*, "Few-shot fault diagnosis of rolling bearing under variable working conditions based on ensemble meta-learning," *Digit. Signal Process.*, vol. 131, p. 103777, Nov. 2022.
[158] Q. Wang *et al.*, "A new DFT-based dynamic detection framework for polygonal wear state of railway wheel," *Veh. Syst. Dyn.*, vol. 61, pp. 1–23, Jul. 2022.
[159] S. Chen *et al.*, "A two-level adaptive chirp mode decomposition method for the railway wheel flat detection under variable-speed conditions," *J. Sound Vib.*, vol. 498, p. 115963, Jan. 2021.
[160] J. He *et al.*, "Defect recognition method for train wheelset tread based on improved SNN", J. China Railw. *Society*, vol. 47, no. 1, pp. 91–100, 2025. (in Chinese)
[161] X. Liu *et al.*, "The wheel flat identification based on variational modal decomposition—envelope spectrum method of the axlebox acceleration," *Appl. Sci.*, vol. 12, no. 14, Art. no. 6837, Jul. 2022, DOI. 10.3390/app12146837.
[162] Z. Jin, D. He, and Z. Wei, "Intelligent fault diagnosis of train axle box bearing based on parameter optimisation VMD and improved DBN," *Eng. Appl. Artif. Intell.*, vol. 110, p. 104713, Apr. 2022.
[163] R. Wang *et al.*, "A reinforcement neural architecture search method for rolling bearing fault diagnosis," *Measurement*, vol. 154, p. 107417, Mar. 2020.
[164] B. Liu *et al.*, "Maintenance scheduling for multicomponent systems with hidden failures," *IEEE Trans. Reliab.*, vol. 66, no. 4, pp. 1281–1292, Dec. 2017.
[165] N. Vafaei, R. A. Ribeiro, and L. M. Camarinha-Matos, "Fuzzy early warning systems for condition based maintenance," *Comput. Ind. Eng.*, vol. 128, pp. 736–746, Feb. 2019.
[166] B. Rahimikelarijani *et al.*, "Imperfect condition-based maintenance strategy for a deteriorating rail track system with multiple competitive failure modes," *J. Transp. Eng. Part Syst.*, vol. 146, p. 4020088, Sep. 2020.
[167] A. Erguido *et al.*, "Reliability-based advanced maintenance modelling to improve rolling stock manufacturers' objectives," *Comput. Ind. Eng.*, vol. 144, p. 106436, Jun. 2020.
[168] P. Jiang *et al.*, "Experimental and numerical study on bogie hunting motion of metro vehicles induced by wheel concave wear," *Veh. Syst. Dyn.*, vol. 63, no. 5, pp. 920–943, May 2025.
[169] L. C. B. Sancho, J. A. P. Braga, and A. R. Andrade, "Optimizing maintenance decision in rails: a markov decision process approach," *ASCE-ASME J. Risk Uncertain. Eng. Syst. Part Civ. Eng.*, vol. 7, no. 1, p. 4020051, Mar. 2021.
[170] P. Zhao, *Research on Efficiency Optimisation of High-Speed Railway EMU Operation and Daily Maintenance. [D]*. Beijing: Beijing Jiaotong University, 2022. (in Chinese)
[171] W. Wang *et al.*, "Study on wheel turning and life cycle of heavy-Haul Railway Freight Cars in China," *Roll. Stock*, vol. 60, no. 1, pp. 116–120, 2022. (in Chinese)
[172] A. Consilvio *et al.*, "Risk-based optimal scheduling of maintenance activities in a railway network," *EURO J. Transp. Logist.*, vol. 8, no. 5, pp. 435–465, Dec. 2019.
[173] X. Lin *et al.*, "Maintenance decision-making framework for train wheels based on multi-dimensional degradation state assessment," *Measurement*, vol. 258, p. 119538, Jan. 2026.
[174] S. García-Méndez *et al.*, "An explainable machine learning framework for railway predictive maintenance using data streams from the metro operator of Portugal," *Sci. Rep.*, vol. 15, no. 1, p. 27495, Jul. 2025.
[175] A. Martins *et al.*, "A new adaptable data-driven model approach for applying predictive maintenance in industrial systems through confidence sphere and the HMM-SVM method," *Results Eng.*, vol. 28, p. 108131, Dec. 2025.
[176] Y. Chen and C. Liu, "Sequential multi-objective multi-agent reinforcement learning approach for predictive maintenance," Feb. 04, 2025, arXiv: arXiv:2502.02071.
[177] H. Zhang *et al.*, "Joint maintenance strategy optimisation for railway bogie wheelset," *Appl. Sci.*, vol. 12, no. 14, Jul. 2022.
[178] Z. Shao *et al.*, "Research on wheel turning controlling polygonal wear development of high-speed EMU wheels," *Locomot. Roll. Stock Technol.*, vol. 61, no. 2, pp. 24–28, 2025. (in Chinese)
[179] Y. Yang *et al.*, "Effect of wheel turning on elimination and evolution of out-of-roundness wear of heavy-Haul locomotive wheels," *J. Mech. Eng.*, vol. 61, no. 14, pp. 184–196, 2025. (in Chinese)
[180] D. Ren *et al.*, "Cause analysis and improvement measures for abnormal turning of locomotive wheels with polygonal wear," *J. Cent South Univ. (Science Technology)*, vol. 50, no. 9, pp. 2317–2326, 2019. (in Chinese)
[181] Y. Huang, B. Zeng, and H. Xie, "Wear analysis and turning optimisation of Haoji HXD1 locomotive wheels," *Railw. Locomot. Car*, vol. 45, no. S1, pp. 73–81, 2025. (in Chinese)
[182] T. Liu *et al.*, "Research and application of locomotive wheel turning model for flange thickening phenomenon," *Electr. Drive for Locomot.*, no. 5, pp. 17–22, 2022. (in Chinese)
[183] D. Cui *et al.*, "Effect of the turning characteristics of underfloor wheel lathes on the evolution of wheel polygonisation," Proc. Inst. Mech. Eng. Part F J. Rail Rapid Transit., vol. 233, no. 5, pp. 479–488, May 2019.